

Investigation of Surface Treatments of Niobium Flat Samples and SRF Cavities by Gas Cluster Ion Beam Technique for Particle Accelerators

A.T. Wu, D.R. Swenson¹, P. Kneisel, G. Wu², Z. Insepov³, J. Saunders, R. Manus, B. Golden, S. Castagnola, W. Sommer, E. Harms², T. Khabiboulline², W. Murayi², and H. Edwards²

Thomas Jefferson National Accelerator Facility, 12000 Jefferson Avenue, Newport News, VA 23606, USA

¹ Epion Corporation, 37 Manning Road, Billerica, MA 01821, USA

² Fermi National Accelerator Laboratory, Batavia, IL 60510, USA

³ Argonne National Laboratory, 9700 South Cass Ave., Argonne, IL 60439, USA

Abstract:

More and more particle accelerators are using Nb Superconducting Radio Frequency (SRF) technology due to the steady progress made during the last few decades in the SRF field. Improvement of the surface treatment of Nb SRF cavities is an indispensable part of the evolution of SRF technology. In this chapter, a study of the surface treatments of Nb flat samples and SRF single cell cavities via Gas Cluster Ion Beam (GCIB) technique will be reported. Beams of Ar, O₂, N₂, and NF₃ clusters with accelerating voltages up to 35 kV were employed in the treatments. The treated surfaces of Nb flat samples were examined by a scanning field emission microscope, a scanning electron microscope equipped with an energy dispersive x-ray analyzer, a secondary ion mass spectrometry, an atomic force microscope, and a 3-D profilometer. The experiments revealed that GCIB technique could not only modify surface morphology of Nb, but also change the surface oxide layer structure of Nb and reduce the number of field emission sites on the surface dramatically. Computer simulation via atomistic molecular dynamics and a phenomenological surface dynamics was employed to help understand the experimental results. Due to its effectiveness at changing the depth and composition of the surface oxide layer structure of Nb, GCIB might be a key to understanding and overcoming the limitations of the high-field Q-slope.

Based on the encouraging experimental results obtained from flat sample study, a novel setup was constructed to allow GCIB treatments of Nb single cell cavities. First results of RF tests on the GCIB treated Nb single cell cavities showed that the quality factor Q of the cavity could be improved substantially at 4.5 K and the superconducting gap value, extracted from RF measurements at different temperatures below superconducting transition temperature, was enhanced by oxygen GCIB treatments. This study indicates that GCIB is a promising surface treatment technique for Nb SRF cavities to be used in particle accelerators.

1. Introduction

Radio frequency superconductivity has matured after several decades of steady progress since the pioneering work began at Stanford University in 1965¹. Nowadays, superconducting radio frequency technology (SRF) based on niobium (Nb) is a popular choice for particle accelerators under construction or to be built in near future such as, for instance, international linear collider (ILC), x-ray free electron laser (XFEL) at DESY, energy recovery linac (ERL) at Cornell University in USA, the new Spiral 2 facility in France, and the isotope separation and acceleration (ISAC) II in Canada. The popularity can be, at least partially, attributable to the improvement in surface preparation of Nb SRF cavities in the past few decades.

Conventionally, buffered chemical polishing (BCP) with hydrofluoric, nitric, and phosphoric acids or electropolishing (EP) with hydrofluoric and sulfuric acids is used as the final step of surface treatments on Nb SRF cavities. However, some limitations on the performance of the Nb SRF cavities prepared by the two techniques have been revealed recently. One limitation is a dramatic reduction in quality factor Q_0 (abbreviated as Q-drop) of Nb cavities treated by either BCP or EP starting at a peak surface magnetic field of 90-100 mT without x-ray production^{2,3}. Another limitation is that the cavity performance scatters a lot and it is not yet possible to consistently achieve high accelerating gradient and high Q_0 . Although the Q-drop can be recovered fully or partially by a low temperature baking at 100-120 °C, it is highly desirable to have Nb SRF cavities that do not show such limitations. In order to achieve this goal, the mechanism responsible for such limitations has to be understood.

It is well known that Nb is a highly reactive metal. When it is in contact with air, an oxide layer of a thickness of about 6 nm is immediately formed on its surface. It is generally believed that a better control over this surface oxide layer structure, chemical composition, smoothness, and defect concentration will contribute to the elimination of the limitations since the typical RF penetration depth for Nb is 50 nm. There are several ways that may eventually lead us to the goal. One promising way in this direction is to fabricate cavities using single or large grain Nb⁴. Others include new surface preparation techniques called buffered electropolishing (BEP)^{5,6} and gas cluster ion beam (GCIB) treatments⁷ where a smoother and chemically modified surface can be obtained. This chapter will focus on the research and development done on Nb flat samples and SRF cavities treated by GCIB technique.

The chapter is organized in the following way: Section 2 gives a brief review of GCIB history and its applications to SRF technology based on Nb. The working principal of GCIB is illustrated in Section 3. Section 4 shows the experimental results of suppression of field emission on the surfaces of Nb flat samples after GCIB treatments as revealed by a scanning field emission microscope (SFEM). The shape, microstructure, and composition of the detected emitters were examined by a scanning electron microscope (SEM) coupled with an energy dispersive x-ray (EDX) analyzer. Possible mechanism of the suppression of field emission is discussed. Section 5 deals with

experimental and computer simulation investigations of the modifications of the morphology of Nb surfaces by GCIB treatments and discusses the implications of the modifications related to the performance of Nb SRF cavities. The change of surface oxide layer structure of Nb after GCIB treatments from the measurements of a dynamic secondary ion mass spectrometry (SIMS) are addressed in Section 6. The first results of RF measurements on the oxygen GCIB treated Nb SRF cavities will be reported in Section 7. Finally summary and perspective are given in Section 8.

2. Brief History of GCIB and Its Application to Nb

The idea of GCIB first came up in 1988 at the Ion Beam Engineering Experimental Laboratory of Kyoto University by I. Yamada according to Reference 8. It was demonstrated in 1991 experimentally that an intense gas cluster beam could be formed at room temperature via supersonic expansion through a nozzle⁹. The gas cluster beam was ionized¹⁰ in 1992 so that GCIB was formally born. For detailed information regarding the evolution of GCIB in general, please see reference 8.

The first commercial GCIB system named Ultra-smoother was made by a Boston-based company called Epion Corporation in 1999. Since then, Epion has sold GCIB systems to companies world wide for microelectronics and related manufacturing and for enhancement of critical surfaces in devices used for data storage, optics, and telecommunications¹¹. Epion Corporation was purchased by Tokyo Electron (TEL) in 2007. TEL is the world's second largest supplier of semiconductor production equipment. The major field for the applications of GCIB is the semiconductor industry. However, development of GCIB technique in Japan and USA in the past decade or so has extended the technology to the applications of many different fields, including surface smoothing of magnetic materials, IC process applications, GCIB-assisted thin film deposition, surface treatments of electrodes, and surface treatments of Nb SRF cavities. These applications are determined by the following two unique properties that GCIB possesses: 1) GCIB has a very low charge to mass ratio. Take Ar GCIB as an example. Typically one Ar cluster contains¹² 10,400 atoms and an average charge of +3.2. Therefore, at a given beam current density GCIB can transport up to thousands of times more atoms than that via a conventional monomer ion beam. 2) The energy that is involved in the interactions between the atoms of a treated surface and the individual atom of a GCIB cluster is low. This is a direct consequence of the first property since the energy of the individual atom of a GCIB cluster is the total energy of the cluster divided by the total number of atoms. For Ar, typical average cluster energy is 64 keV¹². Therefore, the energy of an atom of the cluster is less than 6.2 eV. Consequently, when a GCIB cluster impacts on a surface the interaction is multiple-atoms low energy collisions instead of the simple conventional binary high energy collisions encountered when a monomer ion is employed. These multiple atoms low energy collisions can produce relatively high sputtering, shallow implantation, and other kinds of nano-scale surface modifications¹³ with low mechanical damages to the treated surfaces, which are the important characters required by many applications mentioned above and the application discussed in this chapter.

Application of GCIB to Cu radio frequency (RF) cavities was initiated by D.R. Swenson and coworkers as evidenced in the reference 14 published in 2005 where efforts were made on mitigating high voltage breakdown by reducing the surface roughness of oxygen-free Cu via GCIB. At the 12th SRF Workshop in July 2005, after I gave a talk on the world's only Surface Science Lab (SSL) that was set up at Thomas Jefferson National Accelerator Facility (Jefferson Lab) to study exclusively various surface problems of Nb SRF cavities, I was approached by D.R. Swenson so that a pleasant collaboration on the application of GCIB to Nb was started. At the moment, we were mainly interested in the possible effects of GCIB treatments on the long standing field emission problem on the surfaces of Nb SRF cavities which is still one of the main challenges that our SRF community is facing up to now. As will be shown in the following we found that GCIB treatments could reduce the number of field emitters on the Nb surfaces remarkably. Preliminary results of the study were published in reference 7. Amazed by the results, an effort was made to understand the mechanism of the interactions between various GCIB clusters and Nb via several surface measurement systems¹⁵ available at the SSL and via computer simulation¹⁶ through collaboration between Epion, Jefferson Lab, and Argonne National Lab. Encouraged by the results obtained from flat Nb samples, a system was built at Epion to do GCIB treatments on Nb SRF cavities. RF tests of an O₂ GCIB treated Nb SRF single cell cavities were done at Jefferson Lab first and later at Fermi National Lab. A small flat sample was also mounted to the equator of a Nb SRF single cell cavity and then the cavity was treated in exactly the same way as what was done on the first cavity from Jefferson Lab so as to try to understand the results of RF measurements through surface investigations using various surface instruments. All these experimental results will be reported in details in the sections from 4 to 7.

3. Working Principal of GCIB

The working principal of GCIB is schematically illustrated in Fig.1. Various types of gases can be used for GCIB treatments. The gases can be inert such as Ar, Kr, Xe etc. or chemically reactive such as O₂, N₂, CO₂, NF₃, CH₄, B₂H₆ etc. that may react with the surfaces under treatments depending on what the application one has in mind. After selecting an appropriate gas species, the gas is forced through a nozzle that has a typical pressure of 7.6×10^3 Torr on one side and a vacuum of 7.6×10^{-3} Torr on the other side. Therefore the gas undergoes a supersonic expansion adiabatically that slows down the relative velocity between the atoms of the gas, leading to the formation of a jet of clusters. A typical cluster contains atomic numbers ranging from 500 to 10,000 that are held together by van der Waals forces. A skimmer is then used to allow only the primary jet core of the clusters to pass through an ionizer. The clusters are ionized by an ionizer via mainly electron impacts and the positively charged clusters are electrostatically accelerated via a typical voltage ranging from 2 kV to 35 kV and focused by a beam optics. Monomers and dimers are removed from the beam by a dipole magnet before the beam is neutralized with an electron flood. The aperture in Fig.1 after the neutralizer is used to collect the monomers and dimers. Surface GCIB treatments are done through mechanically scanning an object. Typically, the impact speed of the clusters to the

surface of an object under GCIB treatments is 6.5 km/s, and the current of a gas cluster beam can be as high as 1 mA.

The selection of an appropriate gas species for doing GCIB treatment is very important. When an inert gas is chosen, the major effects on the treated surfaces are smoothing and asperity removal due to lateral sputtering. Chemical gases, on the other hand, can produce some additional effects such as, for instance, doping, etching, and depositing, etc. depending on the properties of the treated object and the gas species selected. Implantation is only limited to the top several atomic layers during GCIB treatments due to the low individual atomic energy. One can also combine the use of different gas species in a specific order for a particular application, although less work has been done in this research direction so far.

For the study reported in this chapter, only Ar, O₂, N₂, and NF₃ were used in the GCIB treatments on Nb. Ar was selected because of its smoothing effect. O₂ GCIB is interesting due to the possible chemical reactions between O₂ and Nb and so is true also for N₂, although in case of using N₂ we were hoping that NbN could be formed on the treated surface since the superconducting transition temperature (T_c) is 16.2 K that is much higher than 9.2 K for Nb. NF₃ is expected to have a relatively higher etching and removal rates on Nb than those from other chemically reactive gas species.

4. Suppression of Field Emission by GCIB Treatments

Field emission¹⁷ from the surfaces of Nb SRF cavities has been a limiting factor for particle accelerators operated at high accelerating gradients of 10-30 MV/m. To overcome this problem, the surfaces of Nb SRF cavities must be free from field emission at surface electric fields that are roughly two times the accelerating gradients. This goal is not easy to achieve since in regular accelerating structures field emission often limits the cavity performance starting at a surface field of 20 MV/m. Heating from field emission increases exponentially with the surface field, leading to a dramatic decrease in the quality factor Q_o of the excitation curves of Nb SRF cavities.

The key here is to produce and maintain a clean surface that does not have micron or submicron particulates, chemical residues, and scratches or other sharp surface features. Various techniques¹⁸ such as, for instance, clean room assembly, high pressure water rinse, ultrasonic cleaning with detergent, and recently dry ice cleaning¹⁹ has been employed to mitigate particulates on the surfaces of Nb cavities. However up to now, field emission is still one of the major issues that the SRF community is facing. In this section, it will be shown that field emission on Nb surface can be significantly suppressed by GCIB treatments.

To investigate the effect of GCIB treatments on field emission on Nb surface, a unique home-made system named SFEM^{15,20} was employed. This system also allows the emitters detected on the Nb surfaces by SFEM to be analyzed by SEM and EDX so that information about the dimensions and compositions of the emitters can be obtained.

The experiment was done in the following way: First standard Nb coupons (a typical sample is shown in Fig.2) were fabricated from the same Nb sheet followed by the standard BCP 112 removal of 150 μm . The arrows in Fig.2 indicate the markings for coordinate identification so that the coordinates of SFEM system can be transformed into the coordinates of our SEM and EDX systems for locating the emitters. Then the samples were cleaned by ultrasonic degreasing and DI water rinsing. The coupons surfaces were blown by dry nitrogen gas afterwards. Then the samples were covered partially via a 25 μm thick stainless steel for GCIB treatments employing O_2 , Ar, and NF_3 . After appropriate GCIB treatments, samples are transferred into SFEM measurement chamber via a load-lock entrance purged with flow nitrogen to prevent contamination on the surfaces of the samples.

Experimental results are shown in Fig.3, Fig.4, and Fig.5. The sample used in Fig.3 was masked into quadrants as shown in the figure. No GCIB treatment was done on the region marked "Unprocessed". "P1" region was treated by Ar. "P1+P2" region was treated by Ar first followed by O_2 . O_2 GCIB treatment was done on "P2" region. The locations of the triangles in these figures show where the emitters are and the height of a triangle indicates how strong the emitter is. The taller a triangle corresponds to the lower on-set field gradient the emitter has. All treated regions showed fewer emitters than the unprocessed quadrant. The number of emitters in each region shows the following trend: $\text{P2} < \text{P1} + \text{P2} < \text{P1} < \text{Unprocessed}$. Comparing these results to a binomial distribution shows less than a 1 in 70 chance that this is a random distribution. It is remarkable to see that in the O_2 treated quadrant there is only one emitter that is located close to the unprocessed region. The measurement also suggests that O_2 treatment is more effective in reduce the number of field emitters.

Encouraged by the first test, another coupon was treated by O_2 GCIB. The result of SFEM scans is showed in Fig.4. In this case, half of the coupon surface was covered. Again a dramatic reduction in the number of field emitters was found on the treated region. By assuming a non-preferential distribution of the emitters on the Nb surface before the treatment, the reduction rate for O_2 is 87.5%. The most important difference between Ar and O_2 is that O_2 is reactive with Nb whereas Ar is not. This inspired us to use a more reactive gas species for treating Nb surface. Reference 21 demonstrated that $\text{NF}_3 + \text{O}_2$ can significantly etch Nb and blunt the angles of the grains that protrude from the surface. Therefore $\text{NF}_3 + \text{O}_2$ was adopted for the next treatment. Fig.5 shows the result of SFEM scans on the Nb coupon where half of the surface was covered. Reduction in field emitter number is again seen for the treated half. The reduction rate is 75.0% that is less than 87.5% for the O_2 treated region.

These results seem to imply that the smoothing effect is not the main reason responsible for the reduction as evidenced from Ar GCIB treatment. Chemical reaction is clearly important. But this does not mean that the more chemical reaction the better since the reduction in field emission is more for O_2 treated region than that in $\text{NF}_3 + \text{O}_2$ treated region. We tentatively attribute the effectiveness of O_2 treatment to the modifications of the surface oxide layer structure on Nb surface as shown later in Section 6. We believe that the following three effects from GCIB treatments

contribute to the reduction in field emission. First effect is the smoothing effect of GCIB treatment. GCIB treatments can remove sharp tips or edges so as to suppress field emission. A typical example is shown in Fig.6. Chemically reactive smoothing effect seems to be more effective in reducing the number of emitters than pure mechanical one does as in the case of Ar. The second effect is the so-called "smashing effect" as shown in Fig.7 where a potential emitter in the oxide treated region was found to be suppressed by the bombardment of O₂ clusters and broke into pieces as if it were stepped on by a heavy sumo wrestler. The third effect is the modification of the surface chemical composition, especially the increase of the thickness of the surface insulating layer of Nb such as in the case of O₂.

SEM and EDX examinations were done on the emitters inside the treated and untreated regions of Figs.4 and 5 hoping to find more clues about the characteristics of the emitters and why some emitters were still active after the GCIB treatments. The results of the measurements are summarized in Figs. 8, 9, 10, and 11. For the untreated region in Fig.4, 14 elements were detected from 24 emitters as shown in Fig.8. The most frequent found elements are S, Fe, Cl, Al, Mg, and Si. It is interesting to notice that S, Fe, Al, and Si are also the most frequent found elements²² in the particulates collected in a filter from high pressure water rinse line for Nb SRF cavities at Jlab. S, Si, Al, and Cl are the most frequent found elements in the particulates¹⁵ collected from the rear side of a vacuum pump line for Nb SRF cavities at JLab. Therefore, it is plausible that the emitters are mostly air-born particles or dusts, and/or residuals from BCP treatment, and/or deposits from rinse water. Fig.9 shows the elements found from the emitters in the treated region in Fig.4. It appears that there is not a correlation between Fig.8 and Fig.9. The sizes of the emitters in the untreated region in Fig.4 range from several tens micron to submicron. Among the 24 emitters detected, the emitters with larger sizes tend to have a lower emission onset field. For instance, the emitter indicated by the red arrow in Fig.4 is shown in Fig.12 where the onset field is 17 MV/m whereas other emitters have onset field at least 89 MV/m with a typical length scale less than 10 μm as shown in Fig.13.

For the untreated region in Fig.5, 15 elements were found from the 40 emitters as shown in Fig.10. Most of the 15 elements were also seen in the untreated region in Fig.4 except Cu, Ag, and Ni, implying therefore that the emitters might originate from the same sources as those for Fig.4. Almost all the elements detected in the untreated region appeared in the treated region as shown in Fig.11 except Ag. This is in agreement with the hypothesis that the field emitters are randomly distributed over the surface of a Nb coupon. Unlike the oxygen GCIB treated sample where only 3 emitters were found in the treated region, here there were 10 emitters. Therefore the chance for all the elements detected in the untreated region to appear in the NF₃ treated region increases substantially. One undesirable feature found in the treated area in Fig.5 was a lot of small niobium oxide particles as shown typically in Fig.14. Those particles were presumably a result of NF₃ bombardment and were not active emitters. Close examine revealed that those niobium particles had very smooth surfaces (see a typical example in Fig.15). They seemed to be embedded in the surface the Nb coupon. The particles are niobium pent-oxides since the oxygen peak intensity in the

open window EDX spectrum (Fig.16) taken at the particle is the same as that (Fig.17) taken on the surface of the Nb coupon. It is plausible that the O₂ GCIB treatment after NF₃ turns these particles from Nb or Nb suboxides into pent-oxides and smoothen their surfaces. This also explains why NF₃+O₂ GCIB treatment has a relatively larger etching rate as discussed in the following section.

It is also interesting to note that most of the active emitters are particulates consisting of more than one metallic or semiconductor elements and Nb itself can be an emitter if it exists as a particle.

5. Modifications of Morphology of Nb Surfaces by GCIB

One of the most important effects from GCIB treatments is the ability to modify the morphology of the surface under treatments. This effect is relevant to the performance of Nb SRF cavities, since smoother inner surface of a Nb SRF cavity tends to give better performance²³. It is also an important factor contributing to the suppression of field emission as discussed above in Section 4. This section will deal with how GCIB treatments can modify the morphology of Nb surfaces. To study this effect, experimentally an atomic force microscope (AFM) and a high precision 3-D profilometer are employed and theoretically computer simulation via atomistic molecular dynamics and a phenomenological surface dynamics is used.

The ability of GCIB treatments for modifying Nb surfaces under the treatments manifests itself via the measurements of etching rates. The etching rates of Nb by NF₃+O₂, Ar, and O₂ has been measured quantitatively²⁴ as shown in Fig.18. NF₃+O₂ has the highest etching rate of 5 nm*cm²/S at 35 kV acceleration voltage. As indicated in Section 4, part of this is due to the sputtering effect that creates some noticeable particles of Nb pent-oxides on the treated surface. Since the etching rate measurements were done using a quartz crystal microbalance method²⁴, the re-deposited Nb pent-oxide particles were not counted in the etching rate calculation. Therefore 5 nm*cm²/S is a conservative estimate towards the lower end of the actual etching rate. No re-deposited particles were found on the surfaces of Ar and O₂ GCIB treated samples, although this observation did not rule out the possibility that some of the removed material might be re-deposited onto the treated surfaces, which may create problems for the performance of Nb cavities (see Section 7 for more details).

Typical examples of profilometer measurements on a NF₃+O₂ treated Nb sample are shown in Figs. 19 and 20 for the untreated and treated halves respectively. In general, NF₃+O₂ GCIB treatment using this particular set of treatment parameters does not make the surface smoother. Typically the RMS of the treated region is 615 nm over an area of 200X200 μm² as compared with 315 nm for the untreated region. The differences in morphology between the treated and untreated regions can also be seen by a CCD camera as shown Figs. 21 and 22. This effect becomes even more apparent for NF₃+O₂ GCIB treatment done on EP treated Nb samples as shown typically in Figs. 23 and 24. It seems that there are some shallow craters generated by NF₃+O₂ GCIB treatment on the treated region. Part of the reason for creating the craters can be due to the larger mass involved in NF₃ clusters. Therefore mechanical impact on the treated surface is much larger

than that when employing much lighter clusters such as, for instance, O_2 . More study is needed in order to optimize NF_3+O_2 GCIB treatments on Nb.

Profilometer measurements on an O_2 treated sample, on the other hand, did not see any clear differences between the treated and untreated regions as shown typically in Figs. 25 and 26. The RMS extracted from the scans varies from location to location and it oscillated around $1.27 \mu m$ depending on where the scans were done. The average RMS didn't correlate with a region regarding whether it was treated by O_2 GCIB. This fact was also supported by CCD images as shown typically in Figs. 27 and 28.

However, we know that O_2 GCIB treatments do etch away materials from Nb surface as shown experimentally in Fig.18. Therefore we tried to do a more detailed study employing an AFM. In this case, a Nb coupon was divided into four quadrants as shown in Fig.29. The region marked "U" means that it was untreated, "P1" means it was treated at 25 kV, "P2" means it was treated at 5 kV, and "P1+P2" means it was treated at 25 kV first followed by treatment at 5 kV. This was inspired by the fact that GCIB treatments with an initial etch rate followed by one or more lower etch rates can minimize the remaining roughness of the final surface and minimize material removal in order to attain a desirable level of smoothness²⁵. AFM measurements were carried out using a Nanoscope IV controller dimension 310™ SPM head. Tapping mode was used in all the observations shown in this Section.

Fig.30 shows typical AFM images obtained on all the four quadrants of the sample with a scanning size of $50 \mu m \times 50 \mu m$. The untreated region is rougher than the rest of the four quadrants. "P1+P2" treated region is indeed smoother than that treated by either "P1" or "P2", which is consistent with the suggestions made in reference 25. It seems that the region treated at 5 kV is a little smoother than that treated at 25 kV.

It is interesting to note here that occasionally emitters were found to be destroyed by the SFEM measurements for both NF_3+O_2 and O_2 cases. A typical example was shown in Fig.31. Measurements on the residue of the emitters showed only niobium oxides. However, we did find some small niobium oxide particles in the neighborhood of the explosive emitters. Those niobium oxide particles were probably a by-product of the explosions and could be new emitters.

To understand the intrinsic mechanism associated with the modifications of morphology on Nb surfaces by GCIB treatments, computer simulations through molecular dynamic modeling were employed. Ar and O_2 were selected as the species for the GCIB clusters. Nb surface that would be treated by GCIB was supposed to be (1,0,0). Assuming that each cluster was multiply charged and contained 429 molecules or atoms, it was found that heavier GCIB species such as Ar could generate larger and deeper craters than those generated by lighter GCIB species on a Nb surface as shown in Fig.32. In the simulation here, the kinetic energy of Ar was assumed to be 125 eV/atom and that of O_2 was 100 eV/molecule. This could explain the results found from the profilometer measurements on the samples treated by NF_3+O_2 as shown in Figs. from 19 to 24.

Smoothing effect by GCIB treatments was demonstrated by modeling a Nb surface containing two types of surface tips with significantly different sizes. One tip was a narrow and tall hill with a typical diameter of a few nm. The other was a wide and short hill having a typical diameter of many tens of nm. Both tips had equal volumes and were schematically shown in Fig. 33a. The total modeled area was in the order of 10^6 – 10^7 Å², and this area was irradiated by up to 1000 30 keV O₂ clusters. The clusters randomly bombarded the whole area of the simulation cell. The cluster dose was in the order of 10^3 – 10^4 cluster/cell. The typical irradiation parameters used for surface smoothing were as follows: cluster ion doses were in the range of 10^{12} – 10^{15} ion/cm², average cluster sizes were in the order of 10^3 atoms or molecules, and the total cluster energies was 30 keV. Displacements of surface particles after the cluster impact were modeled in accordance with the probability, obtained in our molecule dynamic simulation of a single cluster ion impact on a flat or inclined Nb surface.

Fig. 33 demonstrates the results of our mesoscale simulations for Nb surface smoothing. The residual roughness is always defined by the geometry of an individual crater and increases with the increase of the total cluster ion energy. This explains why the region treated at 25 kV in Fig.30 is a bit rougher than that treated at 5 kV. The simulation showed that the narrower hill could be removed by an irradiation dose that was five times lower than that required for the blunt hill. The larger the surface bump is in the horizontal plane, the higher irradiation dose is needed to completely remove the hill and smooth the surface. It is known that the narrower hills have a higher chemical potential than those with a larger diameter. Therefore chemically inactive GCIB surface treatments should remove the narrow hills faster than the wider ones. Computer simulation seems to suggest that the surface smoothing of Nb is mostly done by physical removal of the hills through mechanical interactions between the incoming GCIB clusters and the atoms of the treated surfaces rather than by chemical reaction. For details about this computer simulation study, please read reference 26.

6. Modifications of Surface Oxide Layer Structure by GCIB

It is well known that the performance of Nb SRF cavities depends critically on their surface top layer of about 50 nm deep. The out most layer of any Nb surface is always covered with an oxide layer with a thickness approximately 6 nm. Most of the oxides in this top 6 nm layer are Nb pent-oxides that are dielectric and are generally believed to have no negative effects on the performance of Nb SRF cavities. However, some Nb sub-oxides exist at the interface between the Nb₂O₅ and pure Nb such as, for instance, Nb₂O or NbO or others that may not be superconducting or may be superconducting at lower critical temperatures than that of Nb₂O₅. These sub-oxides can definitely cause RF losses and degrade the RF performance of Nb cavities. It is shown in this section that GCIB treatments can modify the surface oxide layer structure of Nb.

To study the modification of the surface oxide layer structure of Nb by GCIB treatments, a home-made dynamic SIMS system¹⁵ was employed. Ar⁺ was used as the primary ion source. Measurements were done at a vertical incident angle, 2.5 keV, and 85 μA/cm². Both whole

spectrum and depth profile were recorded. Depth profile measurements were done via a method described in reference 27. Nb coupons were treated by NF_3+O_2 , O_2 , and N_2 . Ar was not used since it might create confusions for the interpretation of the experimental results since the primary ion source was Ar^+ .

Fig.34 shows the whole spectra for a Nb coupon of which half was treated by GCIB O_2 and the other half was untreated. Depth profile measurements are shown in Fig.35. From Figs. 34 and 35, we can see the following: 1) The Nb surface is cleaner after the GCIB treatment. Elements such as Na and Ca disappear completely after the treatments, while the intensities of other peaks (apart from Nb and its oxides) reduce. 2) Significant amount of oxygen is introduced to the surface layer of Nb and the thickness of the oxide layer of the treated area is increased as compared with that of the untreated area. The increase in the thickness of the top oxide layer contributes significantly to the suppression of field emission as discussed in Section 4. This is because after O_2 GCIB treatment the particulates are attached to a Nb surface that has a dielectric layer with a thickness more than double than that before the O_2 GCIB treatment, which makes the onset field much higher in order to sustain field emission. The mechanism regarding how O_2 GCIB treatments could increase the thickness of the oxide layer is not completely clear at the present moment, since implantation is expected to be minimal in GCIB treatments as discussed in the previous sections. However, somehow probably O_2 GCIB treatments can enhance oxygen diffusion into the interior of Nb. 3) The cracking patterns of Nb and its oxides change significantly after the treatment. For instance, from the two whole spectra we see that Nb/NbO/NbO₂ is 6/11/1 for the untreated area and 6/22/4 for the treated area. 4) The normalized maximum intensity of the oxygen content is 0.084 higher for the treated area. This is an increase of 13.7% than that of the untreated area. This implies that on the treated area, there can be an oxide layer with an oxidation state of $\text{Nb}_2\text{O}_{5+x}$ ($x>0.5$). It is highly plausible that the extra oxygen atoms exist as interstitial atoms in the amorphous Nb_2O_5 layer. It seems that the treatment is not optimized, since the penetration of oxygen into the Nb surface is much too deep.

To explore the oxygen penetration effect, a Nb coupon was treated with different energies and durations in a way identical to that shown in Fig.29. The treatment duration for "P1+P2" region was twice as much as that for "P1" or "P2" region. Oxygen depth profile data are plotted in Fig.36. Fig.36 tells us that the depth of oxygen penetration depends only on the duration of the GCIB treatment and has nothing to do with the treatment energy inside the energy window selected in this study. Higher treatment energy increases only the maximum intensity of the oxygen peak and its location, implying that probably more interstitial oxygen atoms exist in the Nb_2O_5 layer for the region treated at 25 kV. Therefore, GCIB treatment time has to be optimized in order to create a sharp interface between Nb_2O_5 and pure Nb. This work has not been done yet.

SIMS measurements were also done on NF_3+O_2 and N_2 treated Nb coupons. Their whole spectra are shown in Figs. 37 and 38. Na and K are contaminants from the SIMS measurement chamber. It was a bit of disappointment that no NbN ($T_c=16.2$ K) was seen on the N_2 GCIB treated Nb surface. Some residues of NF_3 were detected from SIMS measurements as shown in Fig.37. But they were

not seen from EDX measurements, implying that the residues existed only on the top several atomic layers. It was interesting to note that NbF^+ and Nb_2N^+ showed up in Fig.37. They might come from some compounds formed through reactions between Nb and NF_3 and these compounds might affect the RF properties of a Nb SRF cavity after the treatment. Oxygen depth profile data for NF_3+O_2 and N_2 are plotted in Fig.39. Surprisingly, both curves for NF_3+O_2 and N_2 are under the curve for the untreated region. The peak location after NF_3+O_2 GCIB treatment moved from 51 S to 25 S, indicating that the thickness of the oxide layer on the surfaces of NF_3+O_2 GCIB treated Nb surface were less than half of the untreated region. On the other hand, the peak location after N_2 GCIB treatment moved from 51 S to 75 S that was a little unexpected although the peak intensity reduced from 0.73 to 0.54. This may imply that N_2 GCIB treatment induces oxygen diffusion in a similar fashion as that after O_2 GCIB treatment. But the diffusion comes at the expense of reduced oxygen stoichiometry for the top Nb_2O_5 layer. Therefore the top oxide layer on the N_2 GCIB treated surface may have a stoichiometry of $\text{Nb}_2\text{O}_{5-x}$ ($x>0$). It yet remains to be revealed how this modification of Nb surface oxide layer structure by N_2 GCIB treatment will affect its SRF properties.

7. GCIB Treatments on Nb Single Cell Cavities

The most exciting part of this study is RF measurements on Nb SRF single cell cavities treated by GCIB. GCIB treatments were done at Epion Corporation using a setup shown in Fig.40. From the flat sample study shown in the previous sections, we know that O_2 GCIB treatments are the most effective in suppressing field emission and in modifying surface oxide layer structure. Unlike NF_3+O_2 , they don't generate noticeable particles on the treated Nb surfaces and they don't react with Nb to form compounds other than niobium oxides. As shown in Section 6, N_2 GCIB treatment does not seem to generate the very desirable higher T_c compound NbN on Nb surface. Therefore naturally O_2 was selected for the initial GCIB treatments on Nb single cell cavities described in this section.

In order to be able to do GCIB treatments on Nb SRF single cell cavities, GCIB beam had to be redirected so that it would hit the inner surface of a cavity. Therefore a beam deflector had to be designed and made before the treatments could be done on a Nb cavity. Fig.41 shows the first deflector used for treating a Nb cavity. A 1.3 GHz Nb single cell cavity was made at JLab and cleaned and pumped down to 10^{-7} Torr and shipped to Epion under vacuum. Then staff at Epion opened the cavity shipping container in Class 10 environment and transferred the cavity into the setup shown in Fig.40. Care was taken to not introduce any particulates into the cavity before O_2 GCIB treatment. After the treatment, the process was reversed and the cavity was RF tested at JLab.

Fig.42 shows the first RF test result on the O_2 GCIB treated Nb cavity right after receiving the cavity from Epion. Strong multipacting was found due to contamination on the treated surface. There were following two candidates that might contribute to the contamination: One was improper handling of the cavity. There were many steps in cavity assembly and disassembly, which all had the potential of contamination. Considered the assembly of the cavity in the clean room at JLab alone as received from Epion. At first the bolts/flanges had to be removed, which could

generate a lot of particles. These particles might migrate into the cavity. The other one was the possible debris created by the GCIB treatment. As illustrated schematically in Fig.41, the sputtered material could be re-deposited on to the treated surface. To check this possibility, a Nb coupon was mounted to a Nb cavity as shown in Fig.43 and then performed the same O₂ GCIB treatment as that was done on the first cavity. After the treatment, the Nb coupon was removed from the cavity for SEM and SIMS measurements. If there were debris created by the GCIB treatment, SEM measurements should be able to see them. Fig.44 shows a typical SEM image, no debris similar to what shown in Fig.14 were found. SIMS oxygen depth profile measurements (see Fig.45) reveal that the oxide layer on the Nb surface is even thicker than the Nb coupon treated independently. According to the study presented in Section 4, this should have helped reduce field emission. Therefore, we rule out the possibility that the multipacting is mainly a result of the debris created by the O₂ GCIB treatment.

To remove the contamination of the first O₂ GCIB treated cavity, high pressure water rinse (HPWR) was employed. Fig.46 shows the result of RF test after the HPWR. The test was limited by quenching at 22.7 MV/m. Field emission was not a problem anymore after the HPWR, implying that the contamination was not intrinsic to the O₂ GCIB treatment and the field emission could be avoided if a better cavity handling procedure was established. Although the first measured excitation curve for the cavity was not that impressive, Q₀ measured at 4.5 k was 7.5×10^8 that was even a little better than that after the low temperature baking at 120 °C for 48 hours --- a procedure commonly used for removing the high field Q slope^{2,3}. Furthermore, the superconducting gap value extracted from Q₀ Vs. 1/T measurement (see Fig.47) for the O₂ GCIB treatment is $\Delta/KT_c = 2.04 \pm 0.01$ that is larger than 1.85 commonly found on Nb SRF cavities after the low temperature baking.

Another Nb SRF cavity of 3.9 GHz from Fermi Lab was treated by O₂ GCIB at 2.5 kV in an identical way as that for the Jlab 1.3 GHz cavity and then followed by a low energy O₂ GCIB treatment at 5 kV. This was inspired by the results discussed in Section 5 where it was shown that the region treated by “P1+P2” was smoother than all the rest of the quadrants. RF test results on the Fermi 3.9 GHz cavity is shown in Fig.48. The excitation curve is much worse than that shown in Fig.46. However, it confirmed that Q₀ at 4.5 k was better than that of the average low temperature baked cavities and superconducting gap value was enhanced after the GCIB treatment as shown in Fig.49.

Therefore our cavity data seem to indicate that the effect of O₂ GCIB treatments to the cavity performance is similar to that for Nb SRF single cell cavities after the low temperature baking at 120 °C for 48 hours. In fact, oxygen depth profile measured on a Nb flat sample baked at 120 °C for 48 hrs in an oxygen environment of 1 atmosphere is quite similar to those obtained on the Nb coupon mounted on the scrap cavity (see Fig.50), although oxygen penetration into Nb interior is even more for the O₂ GCIB treated surface than that for the baked Nb coupon. Observations from transmission electron microscope on the baked Nb coupon²⁸ show that the thickness of the surface oxide layer is 6.98 nm that is a little thicker than 6.76 nm of the unbaked one. This would be consistent with SIMS depth profile measurements shown in Fig.50 if the location of the oxygen peak is assumed to correlate with the thickness of the Nb₂O₅. Then the higher intensity of the oxygen after the peak

indicates a higher concentration of diffused interstitial oxygen atoms in the pure Nb lattice underneath the oxide layer. It appears, therefore, that enhanced superconducting gap structure in the GCIB treated Nb single cell cavities is a result of oxygen diffusion into the pure Nb lattice right underneath the surface oxide layer on the Nb surfaces. Clearly, the pioneer work described in this section shows that the superconducting properties (and thus the performance of Nb SRF cavities) of a Nb surface can be altered through O₂ GCIB treatments. Optimization of the parameters of O₂ GCIB treatments may well lead to improved performance for Nb SRF cavities.

8. Summary and Perspective

This chapter described an initial attempt to treat Nb SRF cavities employing a new surface treatment technique called GCIB. It was shown that GCIB treatment with an appropriate treatment agent could suppress field emission on Nb surfaces by as much as 87.5% through measurements using a home-made SFEM. Detailed analyses on the results from SEM, EDX, 3-D profilometer, and SIMS measurements indentified the following three factors that contributed to the suppression: 1) The smoothing effect from GCIB treatments removed the sharp edges and tips of potential emitters. 2) A "smashing" effect broke potential emitters into pieces and "embedded" them into a Nb surface. 3) An increase in the thickness of the top oxide layer of Nb made field emission more difficult.

The modification of Nb surfaces by GCIB treatments was studies in some details via measurements using a 3-D profilometer and an AFM and computer simulation employing molecule dynamic theory. It was found that GCIB treatments at a high energy about 25 keV using a treatment agent with a much heavier atomic or molecule weight than that of a treated surface could result in a significant amount of debris and the surface thus created after the treatment could be rougher than that before the treatment if not optimized. The later point was supported theoretically via computer simulation. It was verified experimentally that more than one step GCIB treatments with a higher etch rate in the initial step followed by a lower etch rates in the second or more steps could produce a smoother surface finish as proposed in reference 25. Theoretical study by computer simulation revealed that narrower and tall hills on Nb surfaces could be removed by an irradiation dose that was five times lower than that required for blunt and short hills. The larger a surface hill was in the horizontal plane, the higher irradiation dose was needed to completely remove the hill and smooth the surface.

The modification of Nb surface oxide layer structure by GCIB treatments was studies by a dynamic SIMS through measurements of whole spectrum and depth profile. It was found that, in general, GCIB treated Nb surfaces were cleaner than the untreated surface. O₂ GCIB treatments introduced interstitial O atoms to the top oxide layer on Nb surfaces and increased its thickness too. On the other hand, NF₃ GCIB treatments reduced the thickness of the top oxide layer. We found no evidence that N₂ GCIB treatments could produce the desirable NbN on Nb surfaces. Perhaps the most important finding from SIMS measurements was that the thickness of the oxide layer did not depend on how energetic an O₂ GCIB beam was in the energy window studied from 5 keV to 30 keV. The thickness was found to be a function of treatment time, namely a function of GCIB dose mainly.

A setup for doing GCIB treatments on Nb SRF single cell cavities was described. Since GCIB is the first Nb surface etch technique that does not involve water, we hoped that good RF test results could be obtained right after GCIB treatments without the need of HPWR. It turned to be not true for the first attempt described in this chapter. Significant amount of multipacting was encountered in the first RF test. Analyses showed that contamination during the handling of the cavity was an important issue that needed to be addressed. The first cavity treated by O₂ GCIB at 25 keV after HPWR reached an accelerating gradient of 22.7 MV/m before quenching. It was shown that Q_o at 4.5 k was 7.5X10⁸ and superconducting gap value was enhanced for O₂ GCIB treated cavities, similar to or a little better than those obtained on low temperature baked cavities. Our results seem to show that the effect of O₂ GCIB on cavity performance is similar to that after the low temperature baking (120 °C for 48 hours). Oxygen depth profile measurements on a Nb coupon co-processed with the O₂ GCIB treated Nb single cell cavity is similar to that for a Nb sample baked in a flow oxygen environment, implying therefore that oxygen may be responsible for the low temperature baking effect. Further study is needed in order to confirm this. GCIB treatments may be a vehicle for understanding the mechanism responsible for the low temperature baking effect.

It is important to point out here that GCIB treatments on Nb SRF cavities is a completely new R&D field. The research described in this chapter is only a very small part of the whole field. Much work is still needed to be done in order to apply GCIB technique to real cavity production. For instance, a detailed study regarding oxygen penetration vs. dose and how the surface smoothness is affected by treatment energy and dose etc. are still needed. NF₃ has a much higher Nb etch rate. However how to block the sputtered materials it creates is still an issue. In fact, we have designed a more advanced beam deflector as shown in Fig.51. But did not get a chance to test how effective it is to block the sputtered materials. Since GCIB treatments are a Nb surface etching and smoothing technique that does not involve any water, it is expected that the surfaces thus created may be completely different from the conventional ones that are treated by BCP, EP, or BEP in terms of surface oxide layer structure. If optimized, GCIB treatments can be employed as the final step for the surface treatments of Nb SRF cavities. Currently the biggest project is the proposed ILC that will probe for new physics using TeV electron and positron beams. ILC requires approximately 16,000 1-meter-long-nine-cell Nb SRF cavities. A conceptual design for GCIB treatments on a nine-cell NB SRF cavity is shown in Fig.52. Our estimate²⁴ showed that it would take less than 9 hours to remove 50 nm (approximately the skin depth of the RF) from the surface of a cylindrical cavity that was one meter long and 10 cm in diameter by assuming an etch rate of 5 nm*cm²/s that is possible as shown conservatively in Fig.18 for a few gas species studied so far. Thus the entire active volume of a Nb SRF cavity could be removed in a few hours, a time comparable to that required for many of the processing steps now in use.

In conclusion, the pioneer investigation described in this chapter indicates that GCIB technique is a promising nanotechnology for surface etching and smoothing of Nb SRF cavities to be used in particle accelerators.

9. Acknowledgment

A.T. Wu would like to thank Dr. G. Ciovati and other JLab colleagues for help in various ways during the period of this R&D activity. Critical help from Dr. Y. Fadeyeva during the course of writing this chapter and comments from Dr. C. Reece are greatly appreciated.

References:

1. J.M. Pierce et al., Proceedings of the 9th International Conference on Low Temperature Physics, Vol.A Plenum, New York, (1965) P36
2. P. Kneisel et al., Proceedings of the 8th SRF Workshop, Abano, Terme, (1997) P463
3. E. Kako et al., Proceedings of the 8th SRF Workshop, Abano, Terme, (1997) P491
4. P. Kneisel, Proceedings of the 13th SRF Workshop, Beijing, China, (2007) TH102
5. A.T. Wu et al., Applied Surface Science, Vol.253 (2007) P3041
6. E. Wang et al, Proceedings of the 13th SRF Workshop, China, 2007 WEP65
7. D.R. Swenson, A.T. Wu, E. Degenkolb, and Z. Insepov, Nuclear Instruments and Methods in Physics Research, Section B: Beam Interactions with Materials and Atoms, Vol.261 (2007) P630
8. I. Yamada and N. Toyoda, Surface & Coating Technology, Vol.201 (2007) P8579
9. I. Yamada, Proceedings of the 14th Symposium on Ion Source and Ion-Assisted Technology, Tokyo, Japan, (1991) P227
10. I. Yamada, Radiation Effects and Defects in Solids, Vol.124 (1992) P69
11. [http://www.thefreelibrary.com/Tokyo+Electron+\(TEL\)+Acquires+Epion+Corporation.-a0157181015](http://www.thefreelibrary.com/Tokyo+Electron+(TEL)+Acquires+Epion+Corporation.-a0157181015)
12. D.R. Swenson, Nuclear Instruments and Methods in Physics Research, Section B: Beam Interactions with Materials and Atoms, Vol.222 (2004) P61
13. I. Yamada et al, Materials Science and Engineering, R34 (2001) P231
14. D.R. Swenson, E. Degenkolb, Z. Insepov, L. Laurent, and G. Scheitrum, Nuclear Instruments and Methods in Physics Research, Section B: Beam Interactions with Materials and Atoms, Vol.241 (2005) P641
15. A.T. Wu, Proceedings of the 11th SRF Workshop, Germany, 2003 ThP13
16. Z. Insepov et al, Nuclear Instruments and Methods in Physics Research, Section B: Beam Interactions with Materials and Atoms, Vol.261 (2007) P664
17. R.V. Latham, High Voltage Vacuum Insulation: Basic concepts and technological practice Academic Press, London, (1995)

18. H. Padamsee, J. Knobloch, and T. Hays, RF Superconductivity for Accelerators, John Wiley & Sons, Inc. (1998)
19. A. Dangwal et al, Journal of Applied Physics, Vol.102 (2007)P44903
20. T. Wang, C. Reece, and R. Sundelin, Review of Scientific Instruments, Vol.73 (2002) P3215
21. D.R. Swenson et al, Physica C, Vol.441 (2006) P75
22. J. Mammosser and A.T. Wu, Jlab Technote, (2002) Jlab-TN-02-025
23. B. Visentin, Proceedings of the 11th SRF Workshop, Germany, (2003) TU001
24. D.R. Swenson, A.T. Wu, E. Degenkolb, Z. Insepov, AIP Conference Proceedings, Vol.877 (2006) P370
25. <http://www.freepatentsonline.com/6805807.html>
26. Z. Insepov et al, Vacuum, Vol.82 (2008) P872
27. A.T. Wu, Physica C, Vol.441 (2006) P79
28. G. Ciovati, Private Communication.

Figure Caption

Fig.1: Schematic of working principal of GCIB.

Fig.2: Standard Nb flat coupon used for the study described in this chapter. The arrows indicate the markings for coordinate identification.

Fig.3: SFEM plot of field emitters on the surface of a BCP treated Nb coupon. The sample was masked into equal quadrants for treatments with Ar and/or O₂ GCIB or not treated as designated in the figure (see text for more details).

Fig.4: SFEM plot of field emitters on the surface of a BCP treated Nb coupon. Half of the coupon was treated with O₂ GCIB whereas the other half was not.

Fig.5: SFEM plot of field emitters on the surface of a BCP treated Nb coupon. Half of the coupon was treated with NF₃+O₂ GCIB whereas the other half was not.

Fig.6: SEM image taken on an O₂ GCIB treated Nb surface. Two potential emitters as indicated by the arrows were suppressed by the treatment via removing sharp edges and tips.

Fig.7: SEM image taken on an O₂ GCIB treated Nb surface. The arrow indicates a potential emitter being “smashed” into pieces as if it were stepped on by a heavy Japanese sumo wrestler.

Fig.8: Elements of the emitters detected by SEM and EDX on the untreated region shown in Fig.4.

Fig.9: Elements of the emitters detected by SEM and EDX on the treated region shown in Fig.4.

Fig.10: Elements of the emitters detected by SEM and EDX on the untreated region shown in Fig.5.

Fig.11: Elements of the emitters detected by SEM and EDX on the treated region shown in Fig.5.

Fig.12: SEM image of the emitter that had an on-set field of 17 MV/m as indicated by the red arrow in Fig.4.

Fig.13: Typical SEM image for emitters in Fig.4 that had an on-set field higher than 89 MV/m.

Fig.14: SEM image of many niobium oxide particles on a Nb surface treated by high energy NF₃+O₂ GCIB.

Fig.15: Close-up SEM image of two niobium oxide particles on the Nb surface treated by high energy NF_3+O_2 GCIB. The two niobium oxide particles appeared to have smooth surfaces and to be embedded into the surface of the Nb coupon.

Fig.16: Open window EDX spectrum taken on the surface of one of the niobium particle shown in Fig.14.

Fig.17: Open window EDX spectrum taken on the surface of the niobium coupon shown in Fig.14.

Fig.18: Etch rates of Nb treated by NF_3+O_2 , Ar, and O_2 GCIB as a function of acceleration voltage.

Fig.19: Typical profilometer image of $200 \times 208 \mu\text{m}^2$ of an untreated region obtained on a BCP Nb coupon treated by NF_3+O_2 GCIB.

Fig.20: Typical profilometer image of $200 \times 208 \mu\text{m}^2$ of a treated region obtained on a BCP Nb coupon treated by NF_3+O_2 GCIB.

Fig.21: Typical CCD camera photo of an untreated region of a BCP Nb coupon treated by NF_3+O_2 GCIB.

Fig.22: Typical CCD camera photo of a treated region of a BCP Nb coupon treated by NF_3+O_2 GCIB.

Fig.23: Typical CCD camera photo of an untreated region of an EP Nb coupon treated by NF_3+O_2 GCIB.

Fig.24: Typical CCD camera photo of a treated region of an EP Nb coupon treated by NF_3+O_2 GCIB.

Fig.25: Typical profilometer image of $200 \times 208 \mu\text{m}^2$ of an untreated region obtained on a BCP Nb coupon treated by O_2 GCIB.

Fig.26: Typical profilometer image of $200 \times 208 \mu\text{m}^2$ of a treated region obtained on a BCP Nb coupon treated by O_2 GCIB.

Fig.27: Typical CCD camera photo of an untreated region of a BCP Nb coupon treated by O_2 GCIB.

Fig.28: Typical CCD camera photo of a treated region of a BCP Nb coupon treated by O_2 GCIB.

Fig.29: A Nb coupon was masked into equal quadrants for treatment with high and low energies O₂ GCIB (see the text for more details)

Fig.30: Typical AFM images of 50X50 μm² obtained on the sample shown in Fig.29. a) for untreated region, b) for "P1" treated region, c) for "P1+P2" treated region, and d) for "P2" treated region.

Fig.31: Typical SEM image of an emitter that was destroyed by SFEM scans.

Fig.32: Craters formed on the surface of (100) Nb treated with a) clusters of 429 Ar at 125 eV/atom, and b) clusters of 429 O₂ at 100 eV/molecule, as calculated by computer simulation via molecular dynamics.

Fig.33: Results of mesoscale modeling of a Nb surface irradiated by O₂ cluster ion beam at a dose of 10¹³ ions/cm². The cluster energy was 30 KeV and the cluster size was about 3000 oxygen molecules in a cluster. The surface contained two types of features: narrow and tall and wide and short (represented in a)).

Fig.34: Typical SIMS whole spectrum measurements done on a) untreated region of a BCP Nb coupon treated by O₂ GCIB and b) treated region of a BCP Nb coupon treated by O₂ GCIB.

Fig.35: Typical SIMS depth profile measurements done on a BCP Nb coupon treated by O₂ GCIB.

Fig.36: Typical SIMS depth profile measurements done on the BCP Nb coupon shown in Fig.29. a) shows close-up plots of the depth profile data. b) shows the depth profiles measured on every quadrant.

Fig.37: Typical SIMS whole spectrum plot for the surface of a NF₃+O₂ treated BCP Nb coupon.

Fig.38: Typical SIMS whole spectrum plot for the surface of an N₂ treated BCP Nb coupon.

Fig.39: Typical SIMS depth profile data obtained on the surfaces of NF₃+O₂ and N₂ GCIB treated BCP Nb coupon. b) is close-up plots of the peaks.

Fig.40: Test stand used for performing O₂ GCIB treatments on single cell Nb SRF cavities. a) shows the schematic of the setup. b) shows the photo of the actual setup.

Fig.41: Schematic of the first GCIB beam deflector used for treating Nb SRF single cell cavities.

Fig.42: Excitation curve at 2 K for the O₂ GCIB treated 1.3 GHz Nb SRF single cell cavity right after the treatment.

Fig.43: Photo of a standard Nb coupon (see Fig.2) mounted on a Nb SRF single cell cavity (scrap cavity) that was treated by O₂ GCIB in an identical way as that for the first Nb SRF single cell cavity.

Fig.44: Typical SEM image of the surface of the Nb coupon co-processed with the Nb scrap cavity by O₂ GCIB. No noticeable particulates from the GCIB treatment were found on the surface.

Fig.45: Typical SIMS depth profiles measured on a Nb coupon co-processed with the Nb scrap cavity. A and B represent the measurements done at two randomly selected locations on the surface. Also included in the plot is the depth profile data shown in Fig.35 for comparison.

Fig.46: Excitation curve at 2 K for the O₂ GCIB treated 1.3 GHz Nb SRF single cell cavity after high pressure water rinse.

Fig.47: Residual resistance measured as a function of 1/T on the O₂ GCIB treated 1.3 GHz Nb SRF single cell cavity.

Fig.48: Excitations curves at 2 K for the O₂ GCIB treated 3.9 GHz Nb SRF single cell cavity before and after the treatment. Also included in the plots is the radiation counts.

Fig.49: Residual resistance measured as a function of T_c/T on the O₂ GCIB treated 3.9 GHz Nb SRF single cell cavity. Also included in the plot is the fit by BCS theory.

Fig.50: Comparison of the SIMS depth profiles for the Nb coupon co-processed with the Nb scrap cavity with that from a Nb sample baked at 120 °C for 48 hrs in oxygen environment of one atmosphere.

Fig.51: Schematic of an advanced design for the GCIB beam deflector with a liner to collect debris created by GCIB treatments.

Fig.52: Conceptual design for a GCIB system for treating a multi-cell Nb SRF cavity.

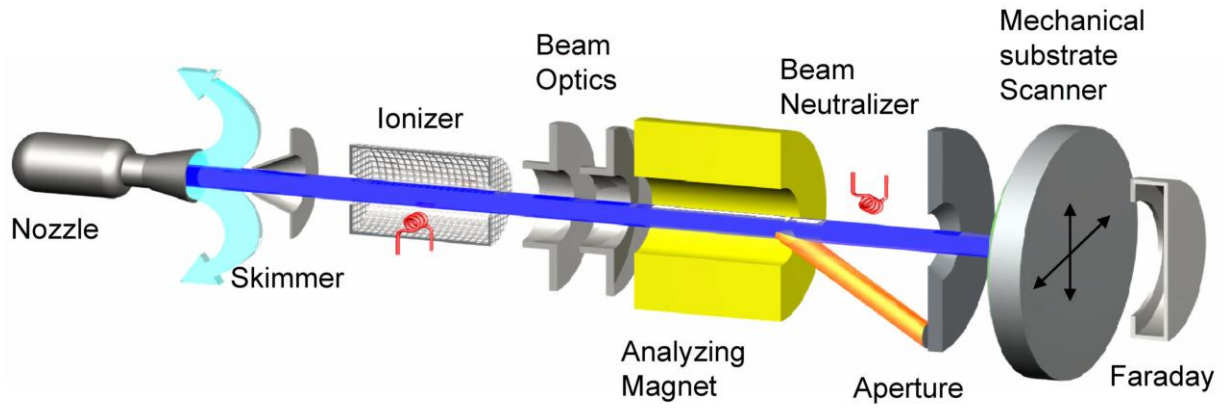


Fig.1

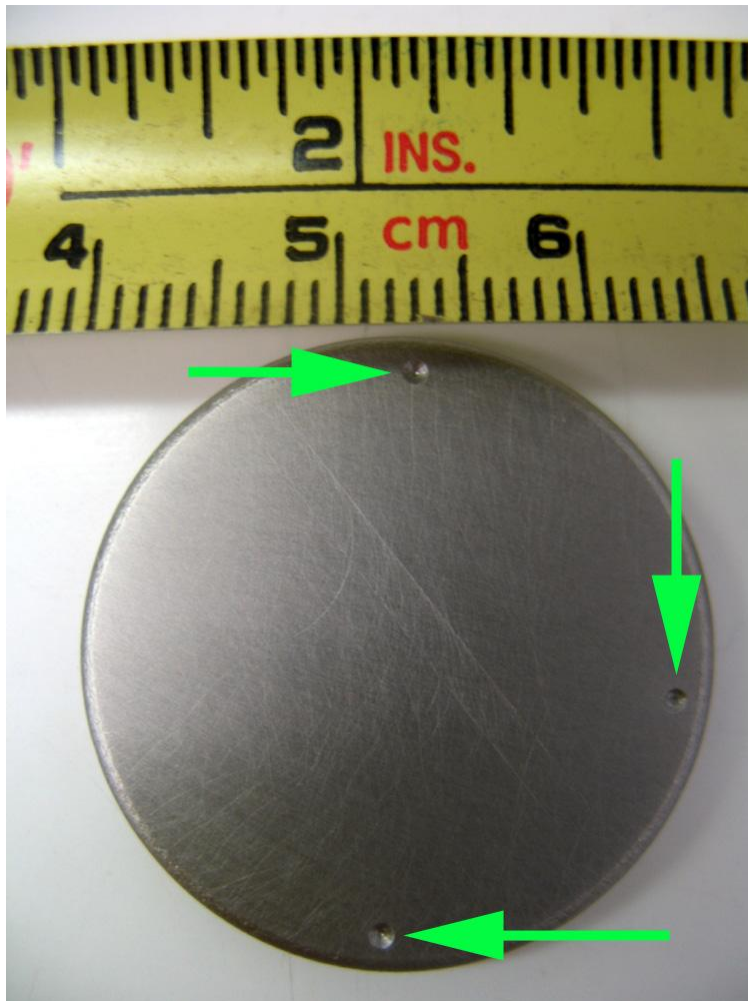


Fig.2

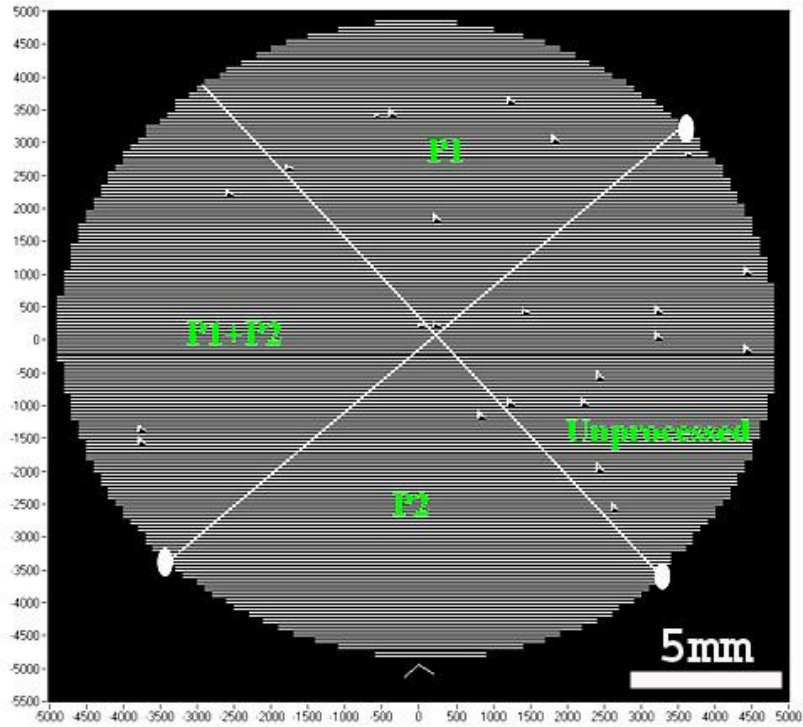


Fig.3

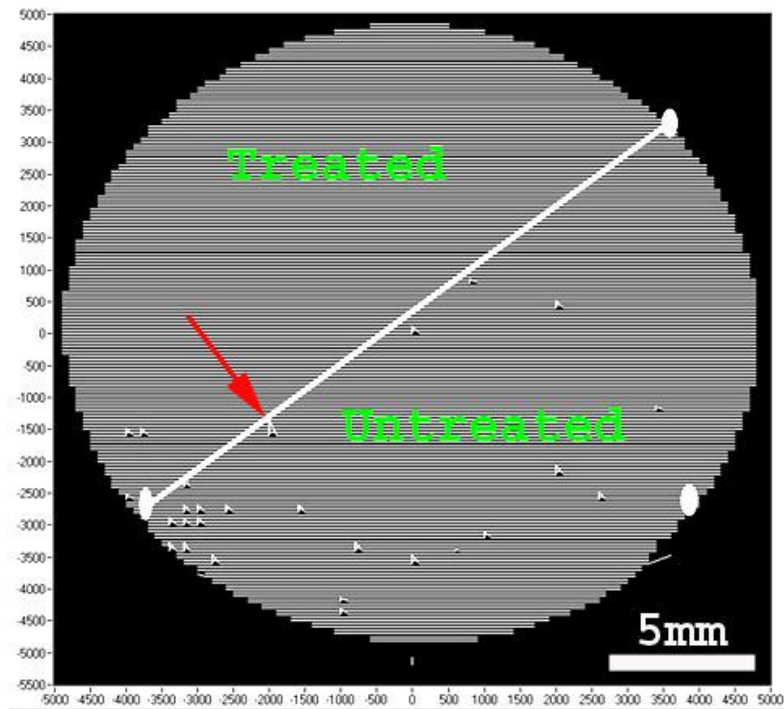


Fig.4

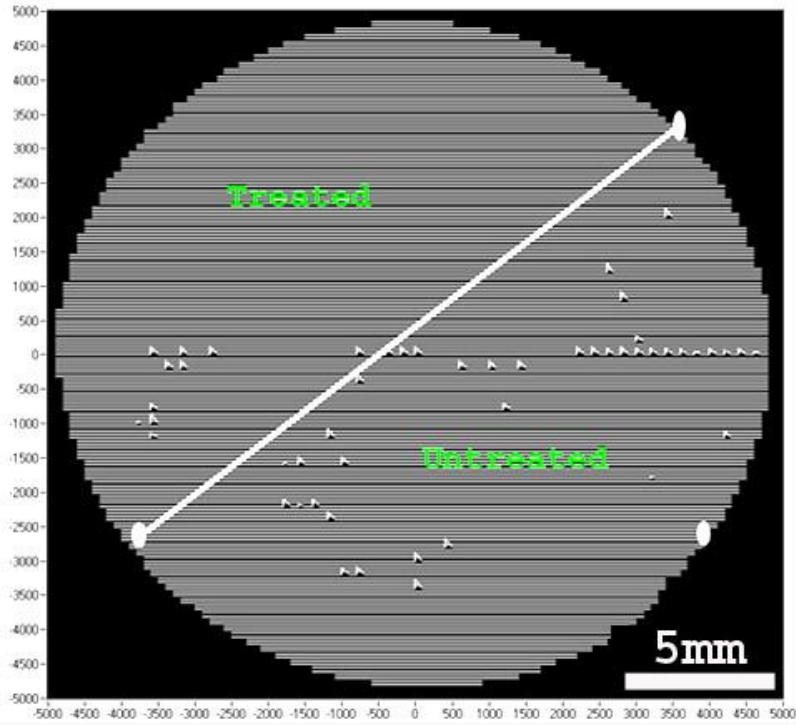


Fig.5

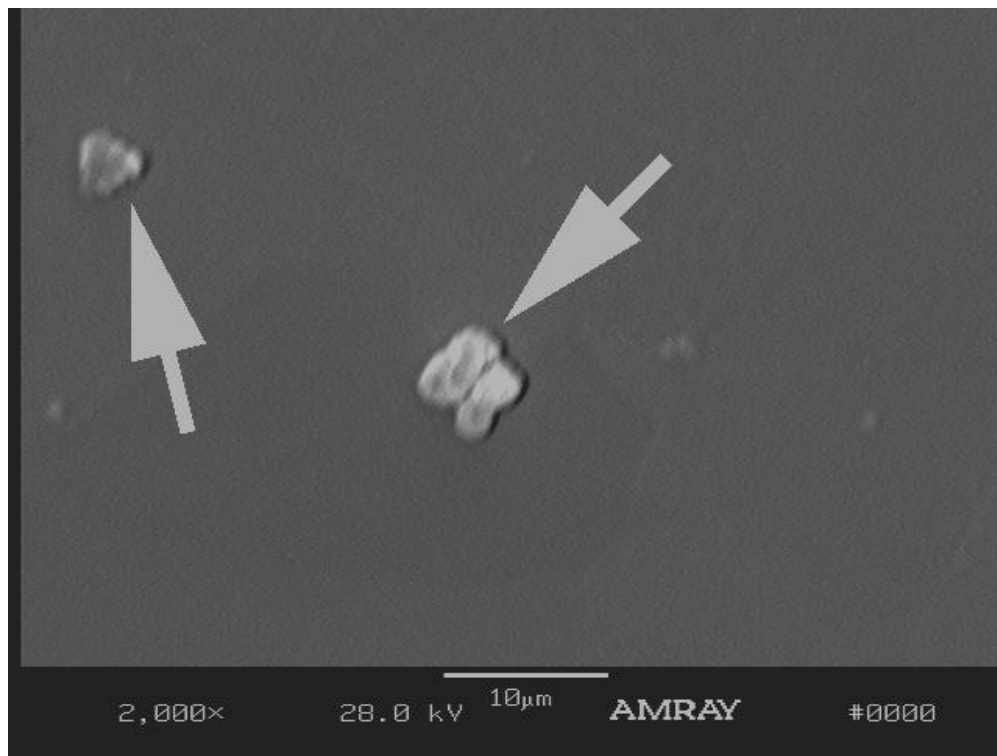


Fig.6

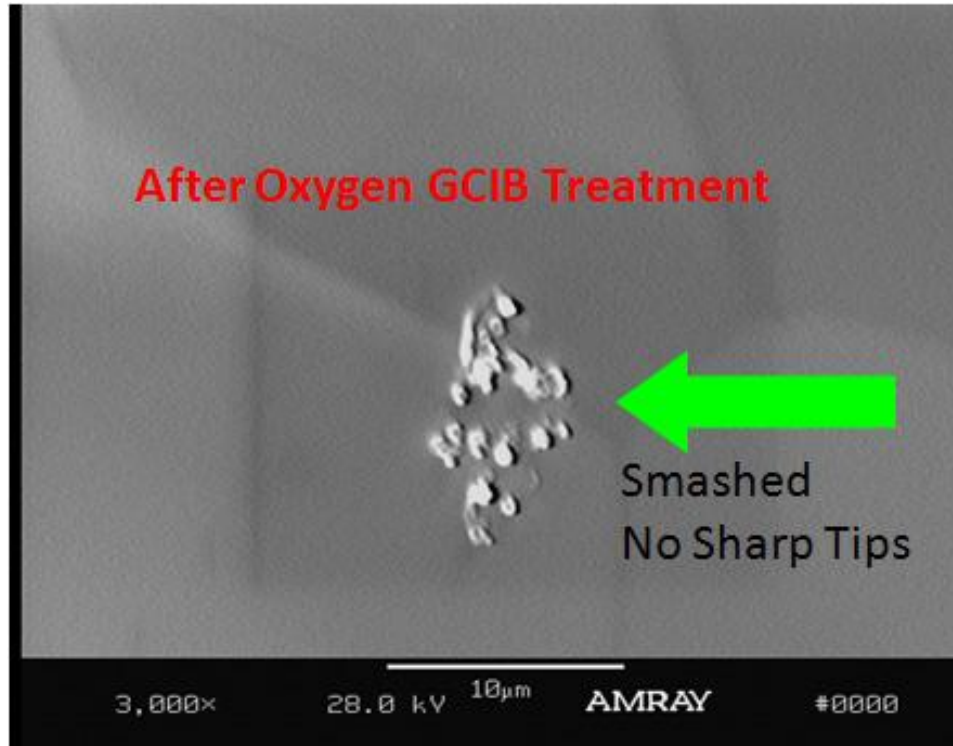


Fig.7

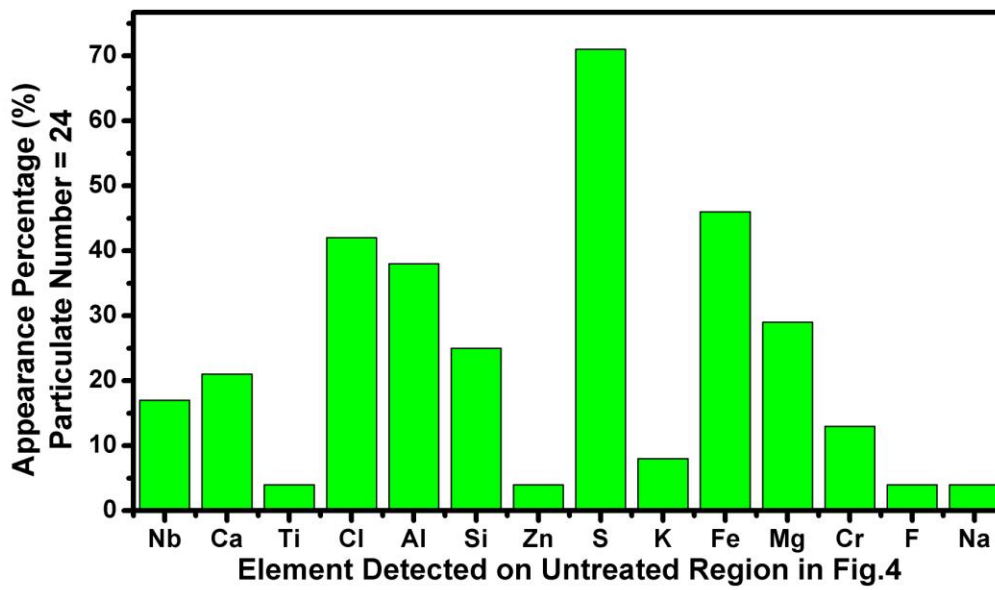


Fig.8

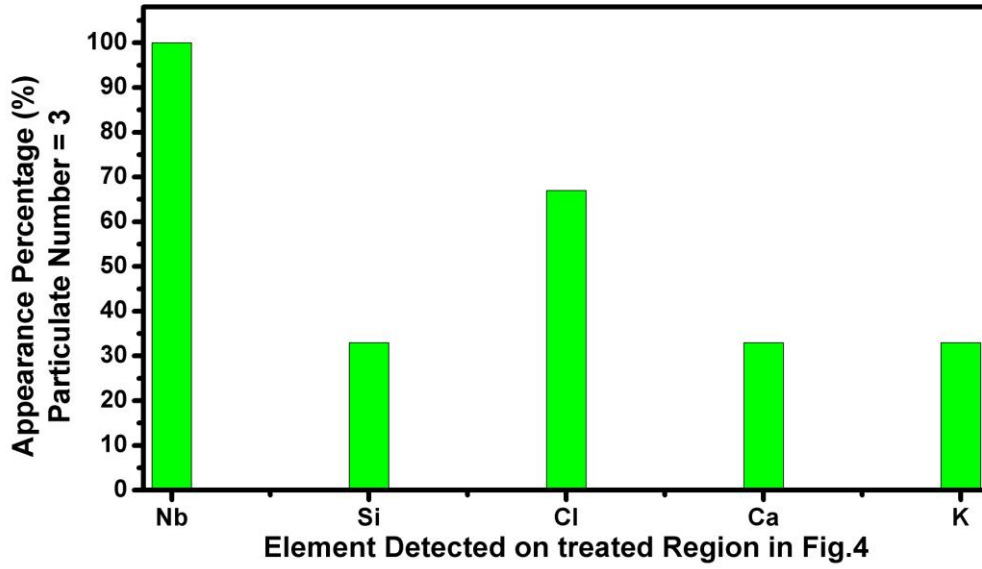


Fig.9

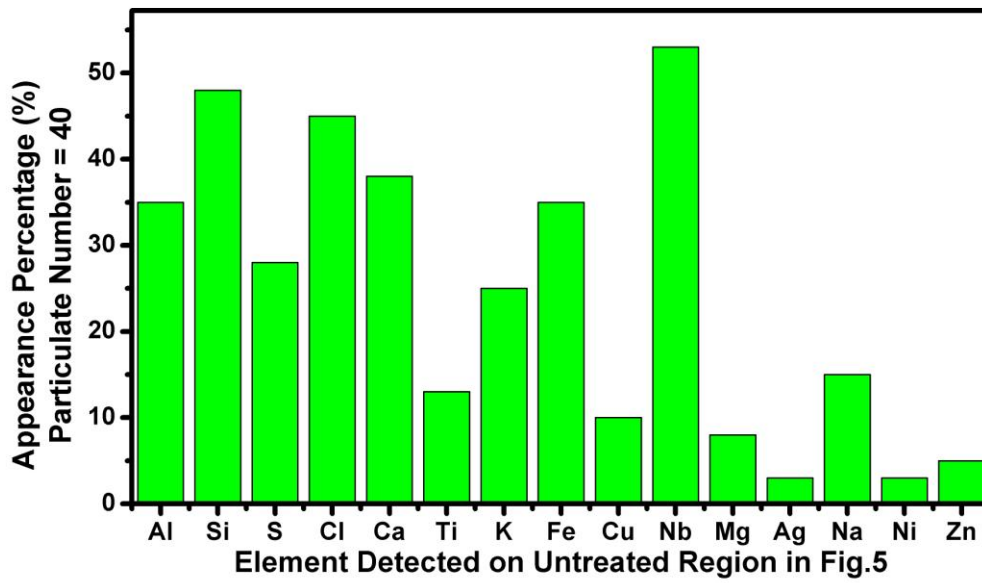


Fig.10

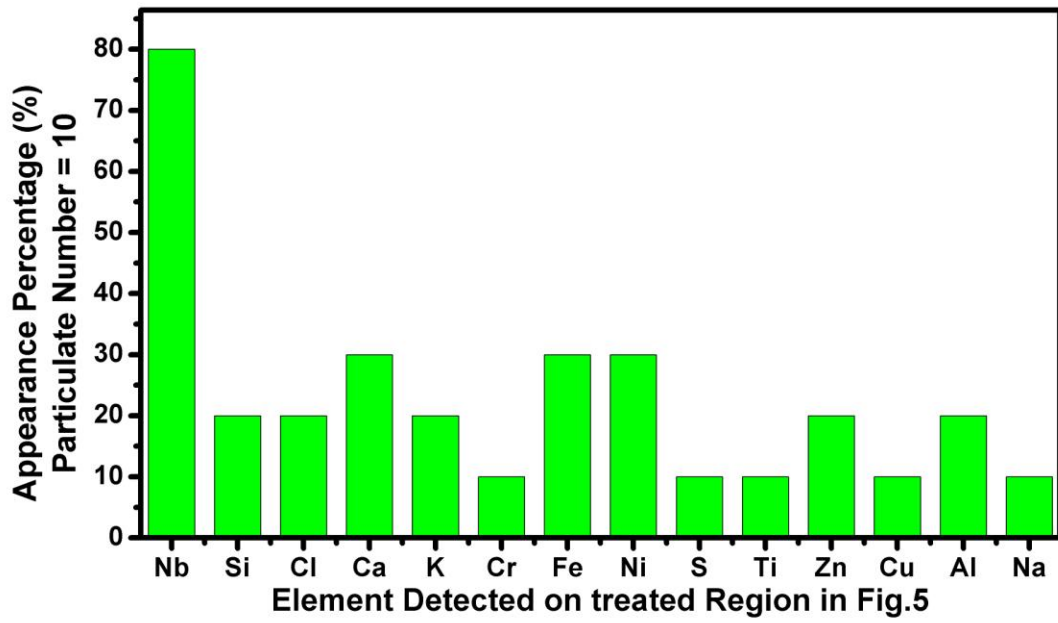


Fig.11

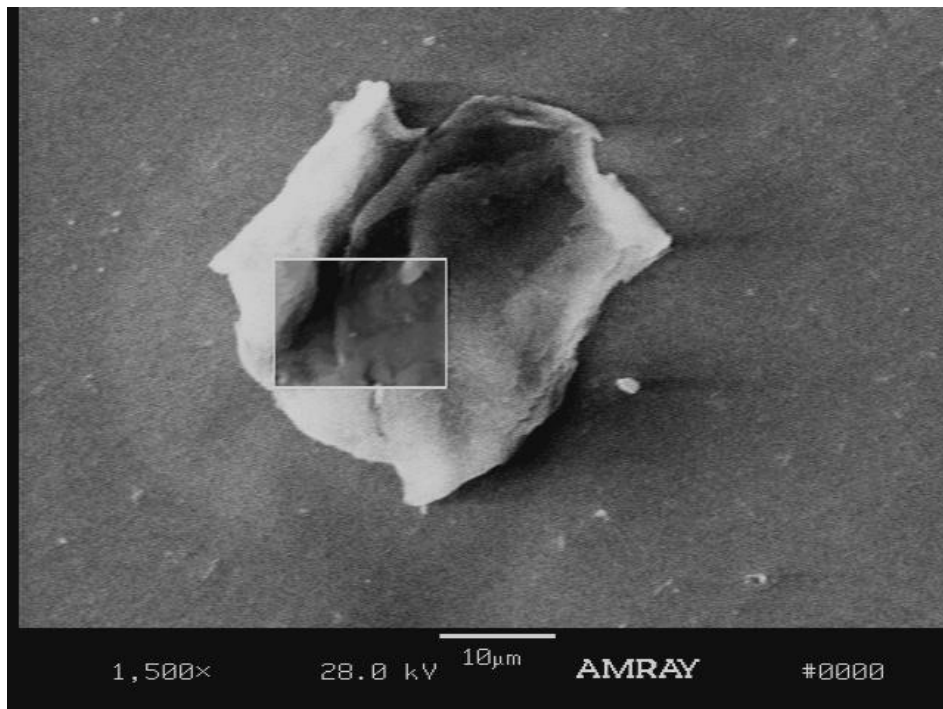


Fig.12

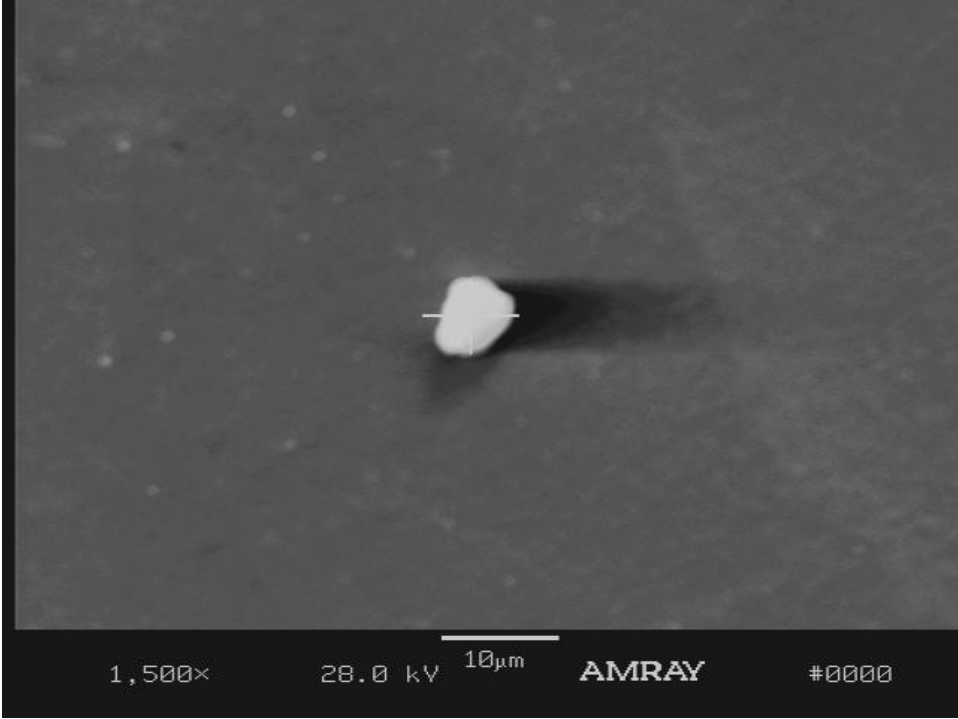


Fig.13

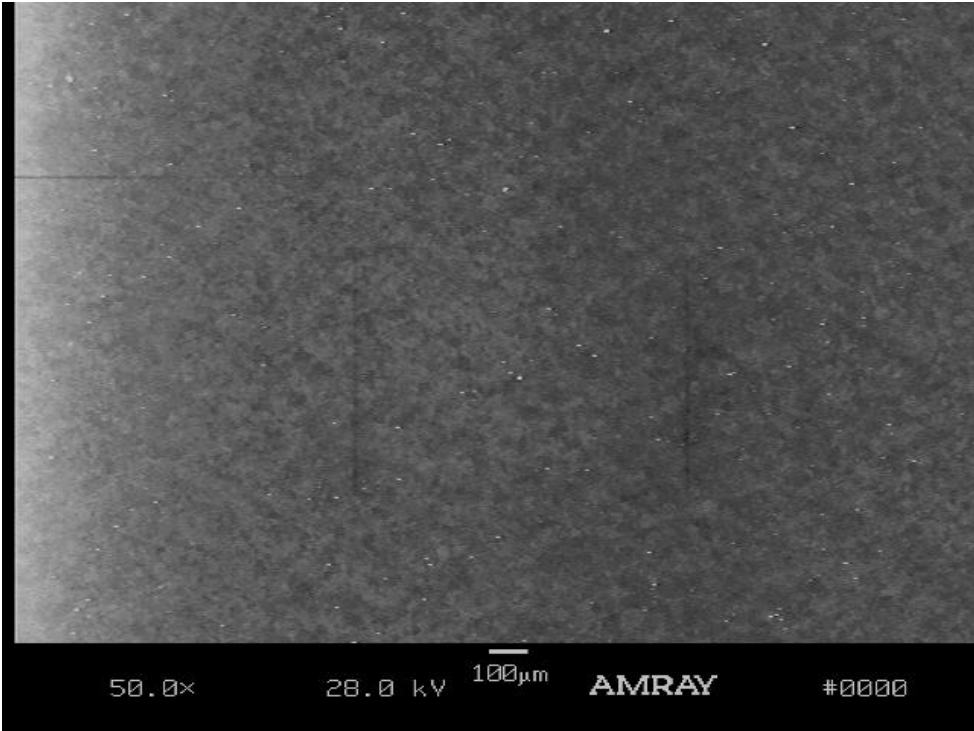


Fig.14

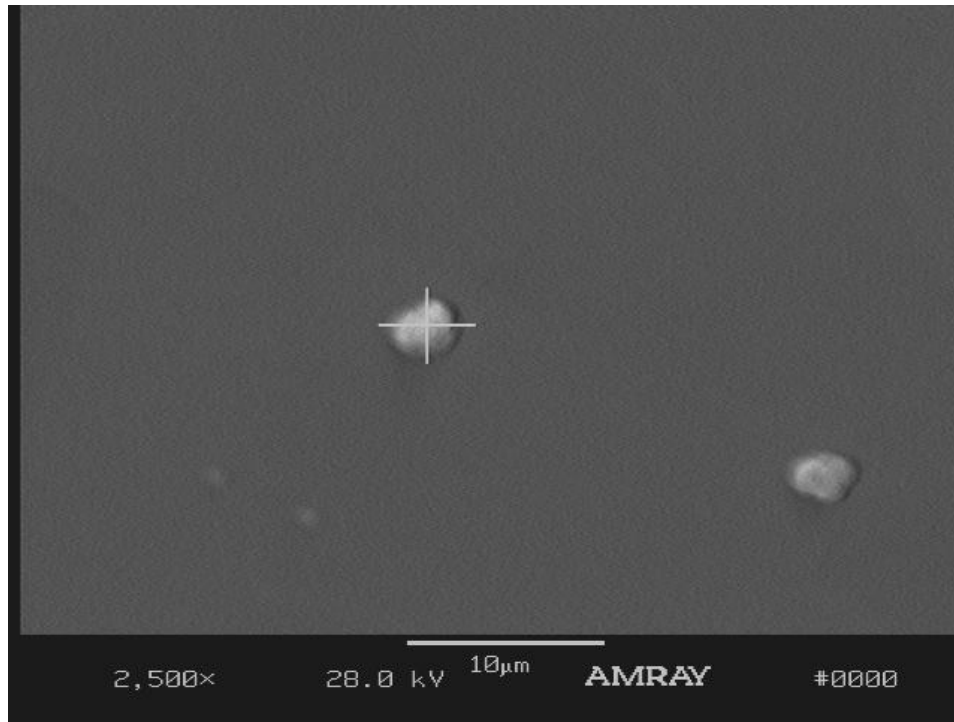


Fig.15

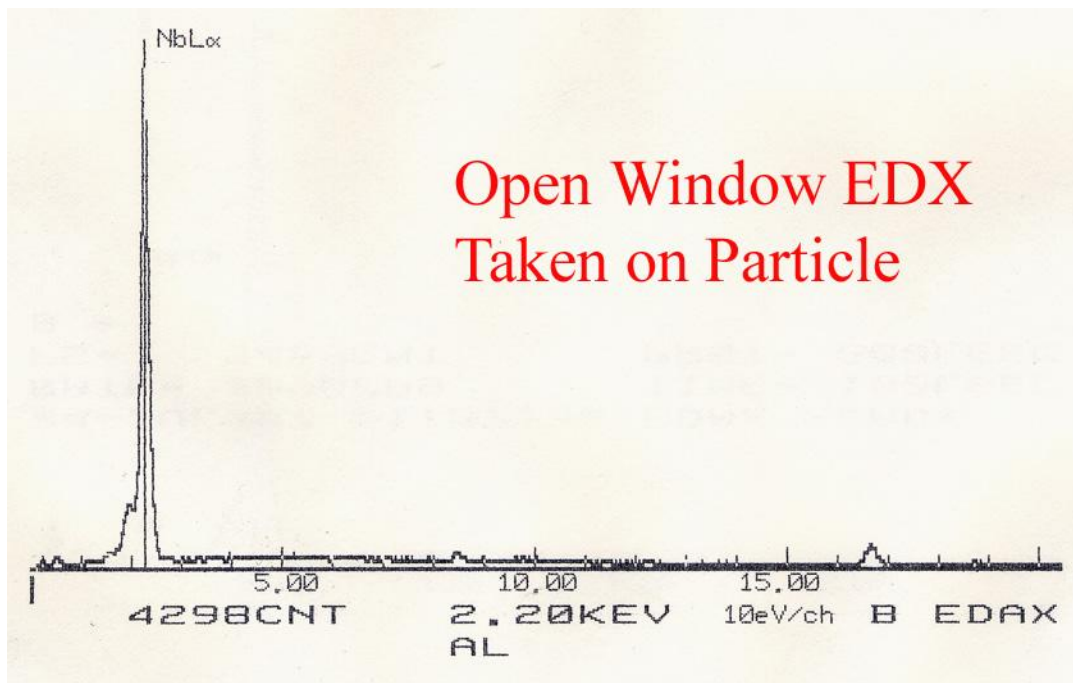


Fig.16

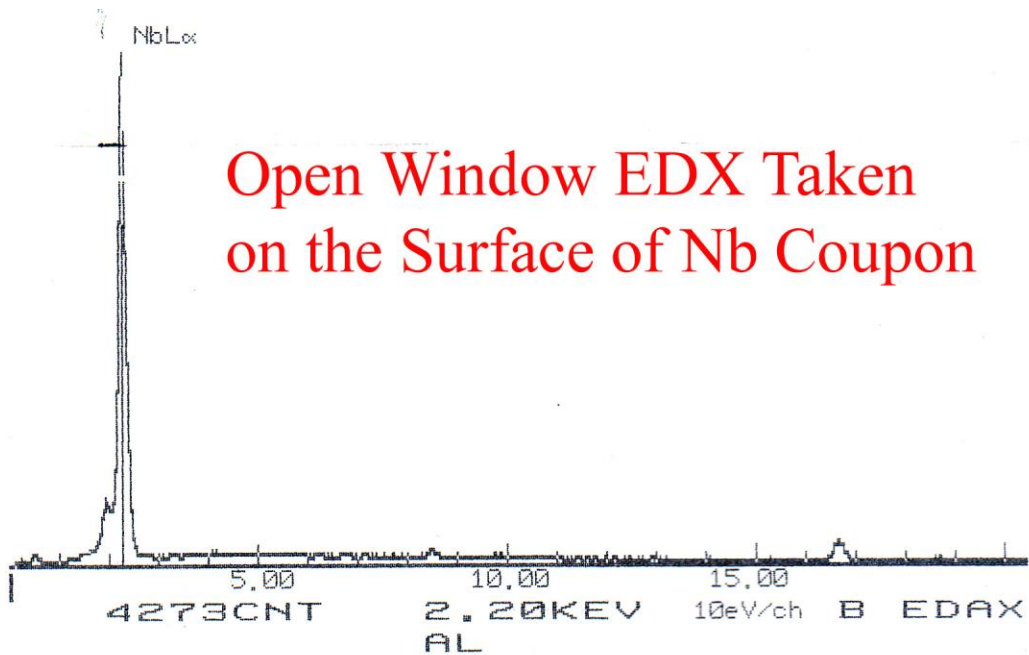


Fig.17

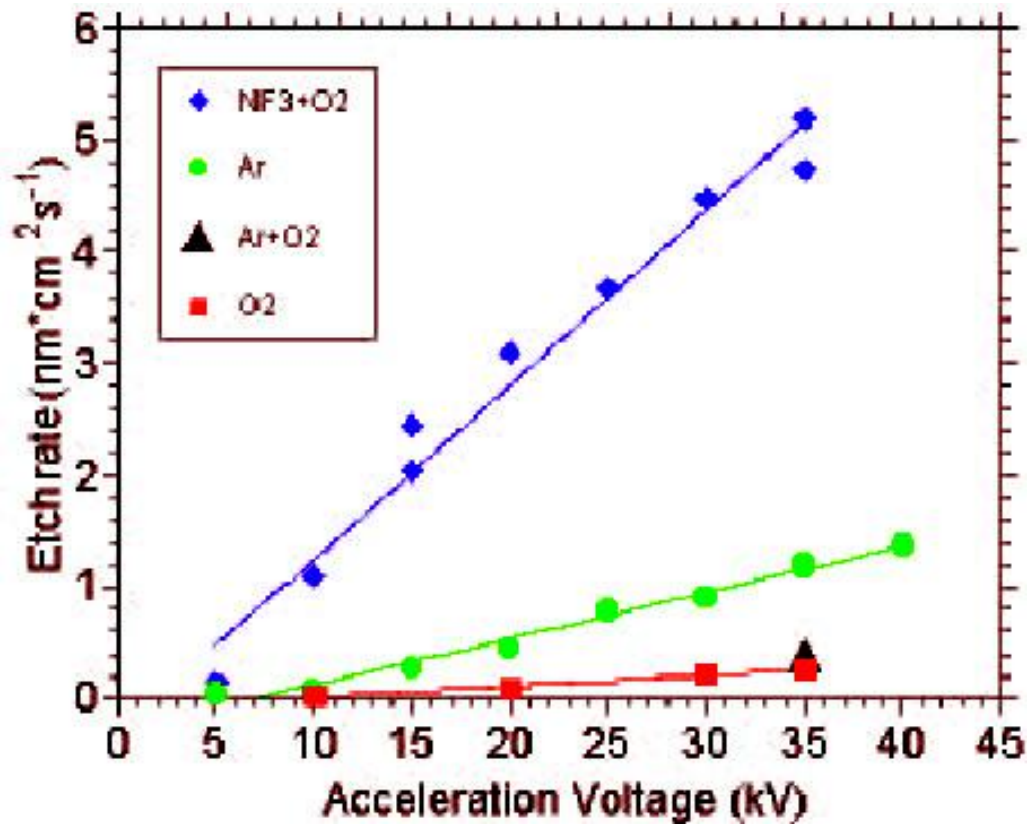


Fig.18

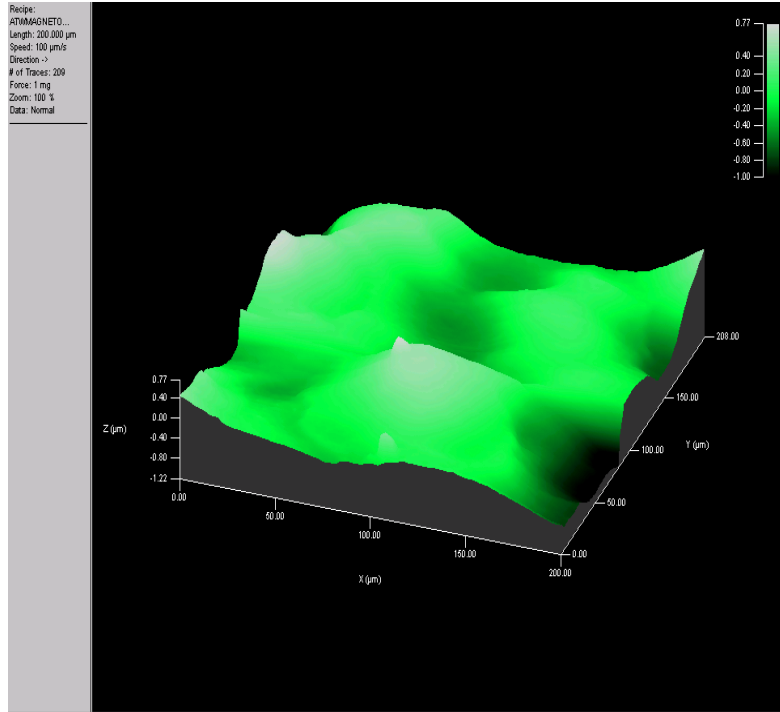


Fig.19

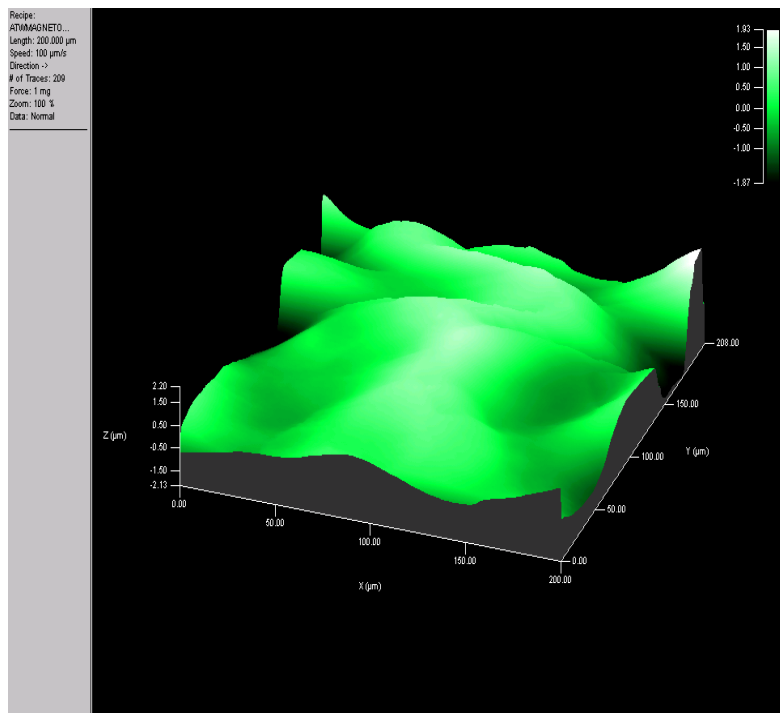


Fig.20

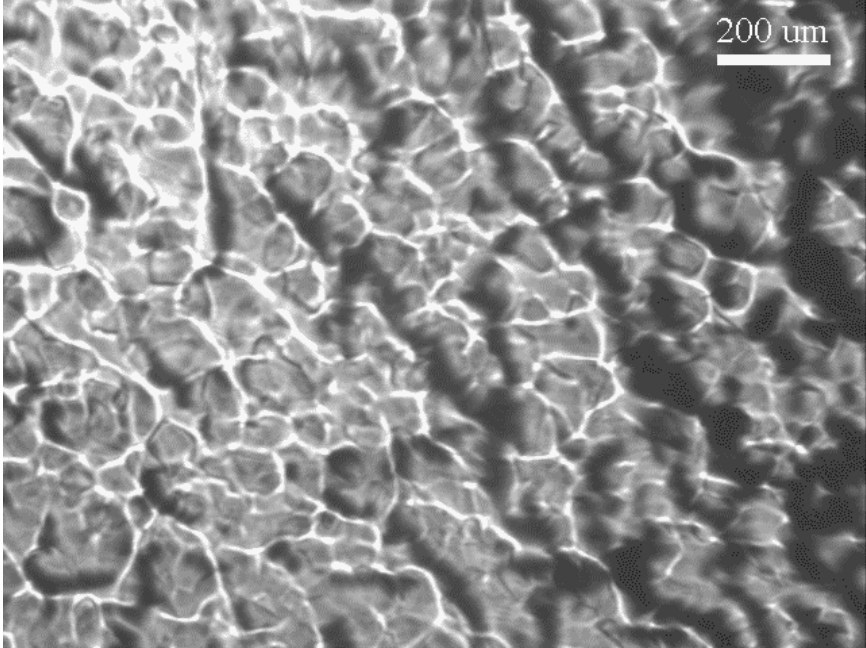


Fig.21

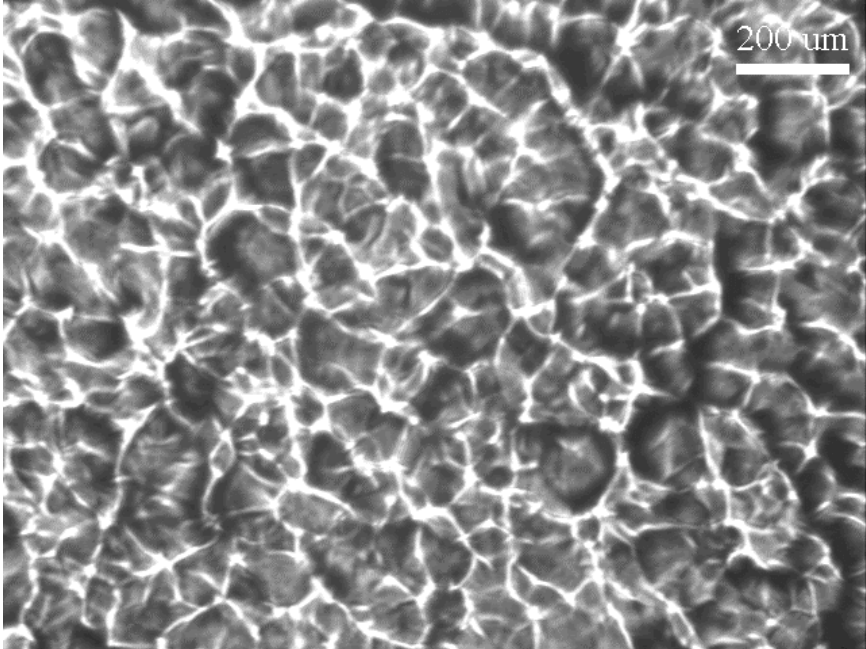


Fig.22

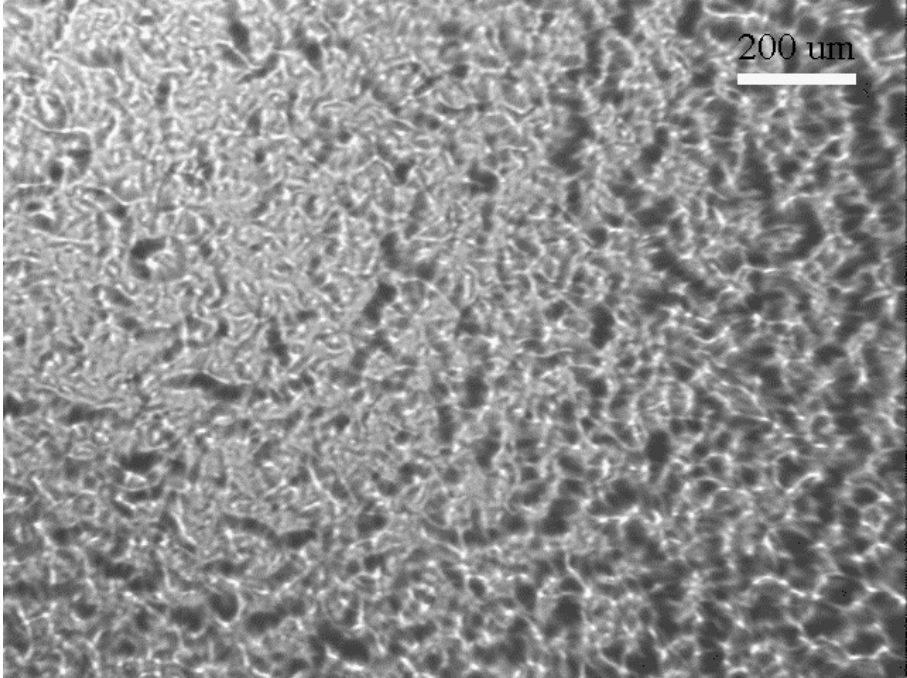


Fig.23

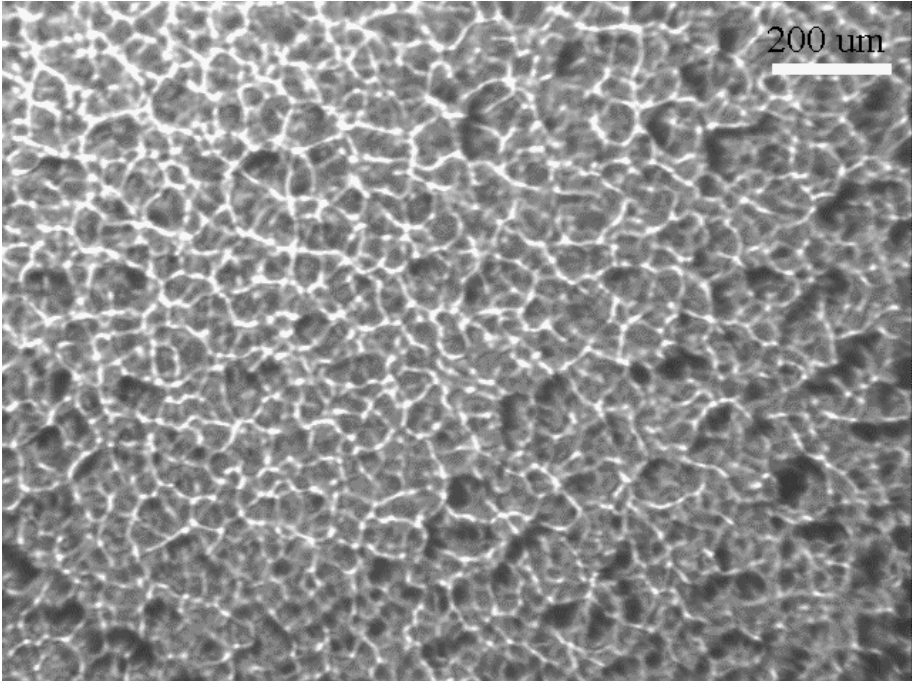


Fig.24

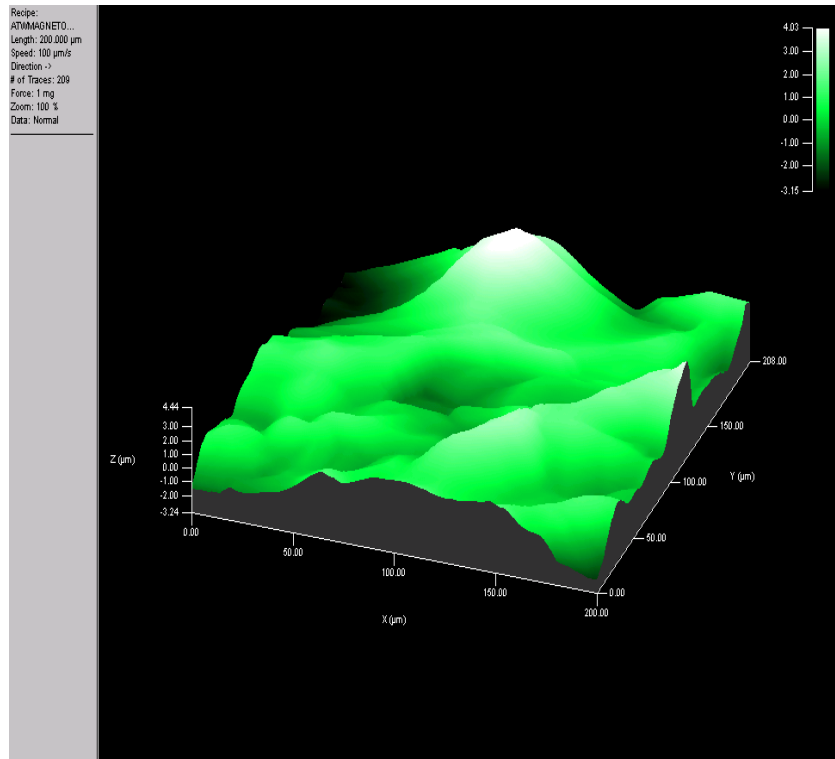


Fig.25

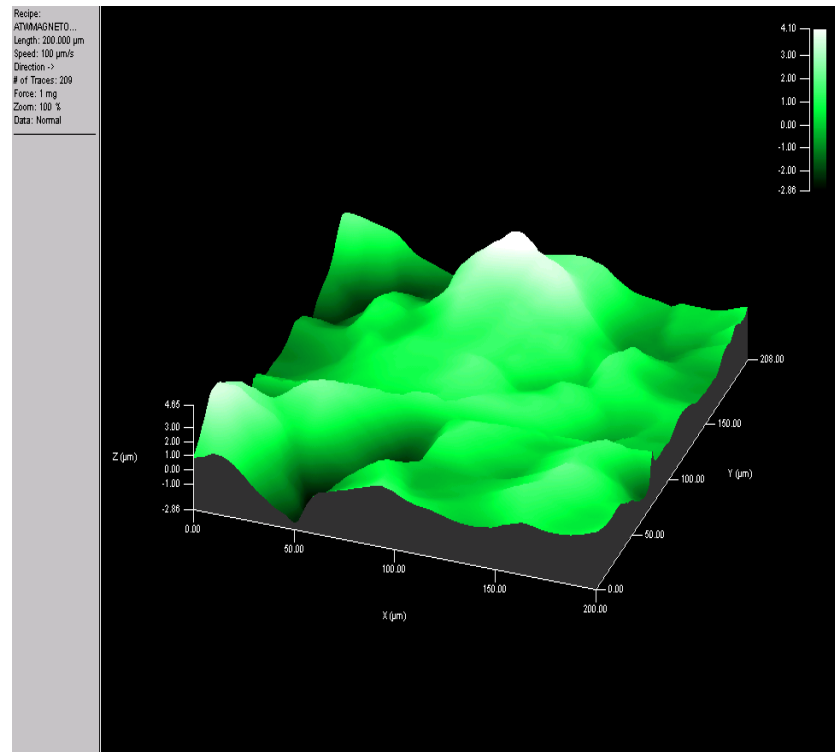


Fig.26

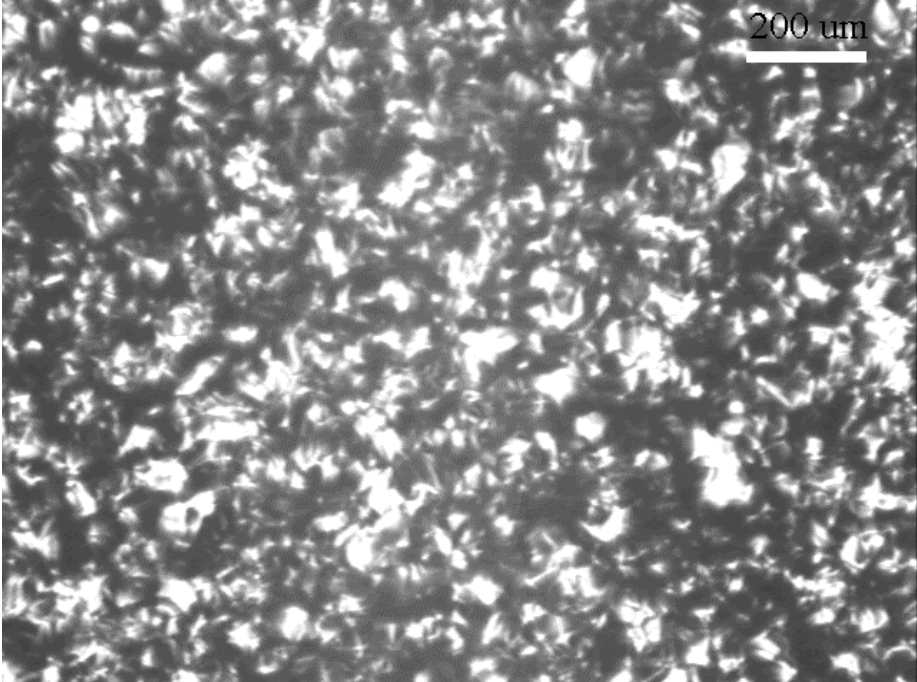


Fig.27

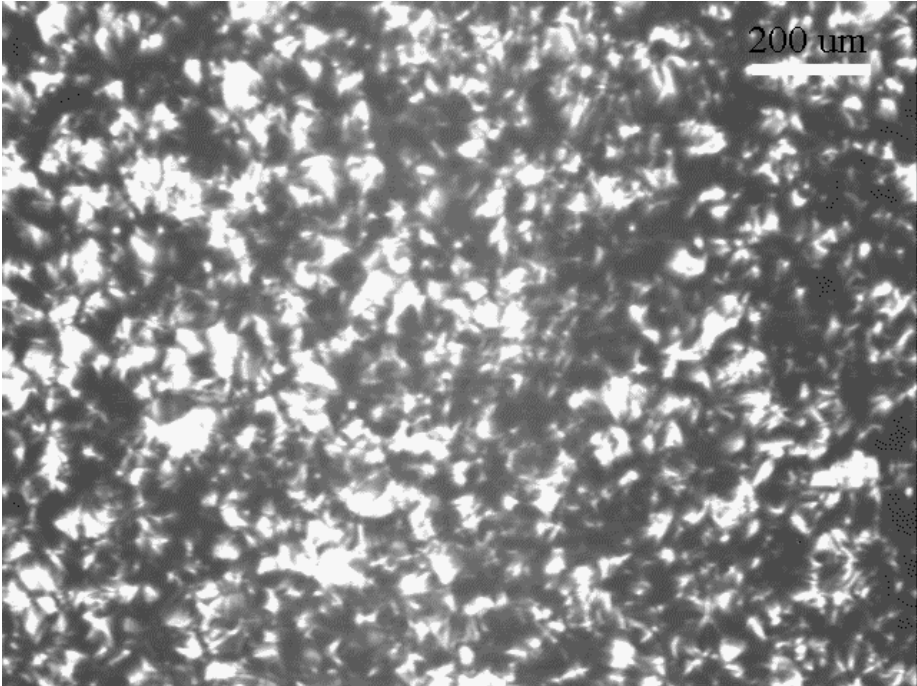


Fig.28

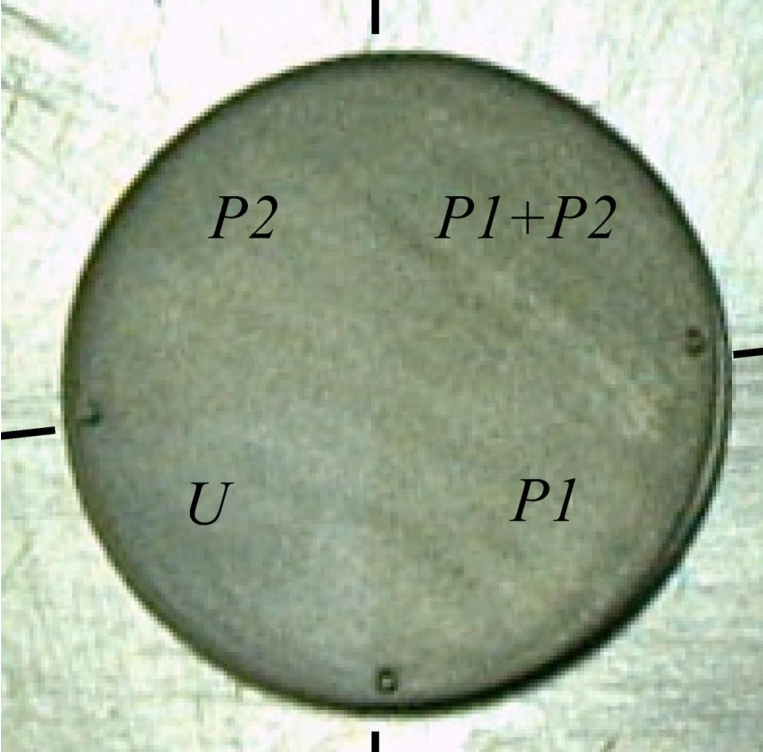


Fig.29

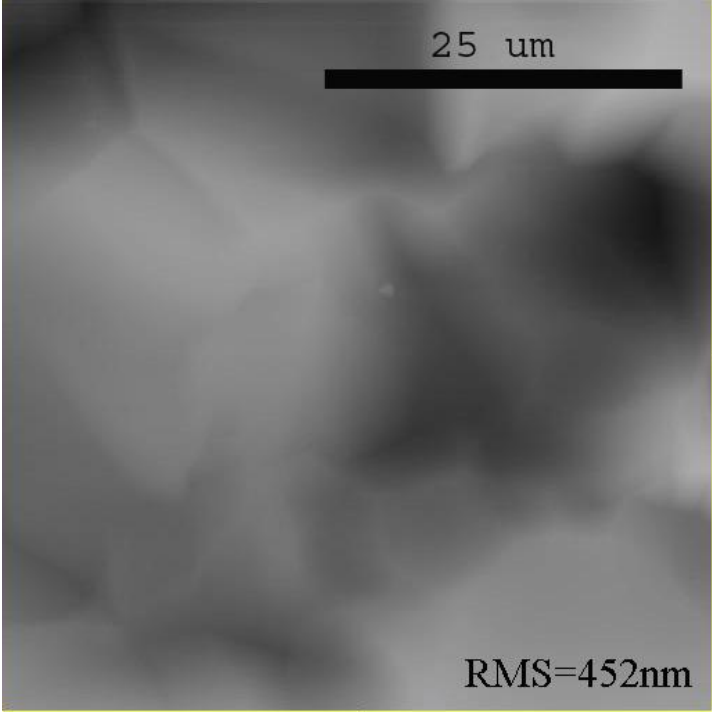


Fig.30a

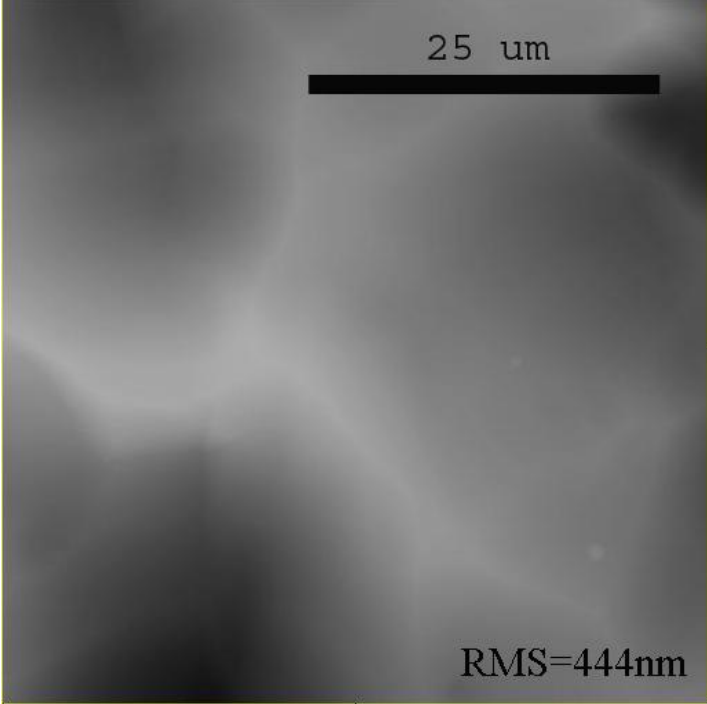


Fig.30b

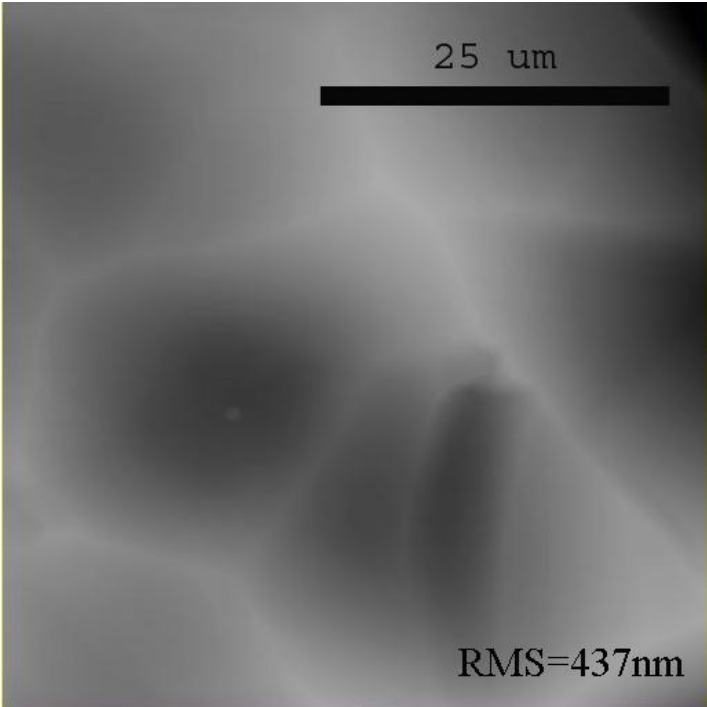


Fig.30c

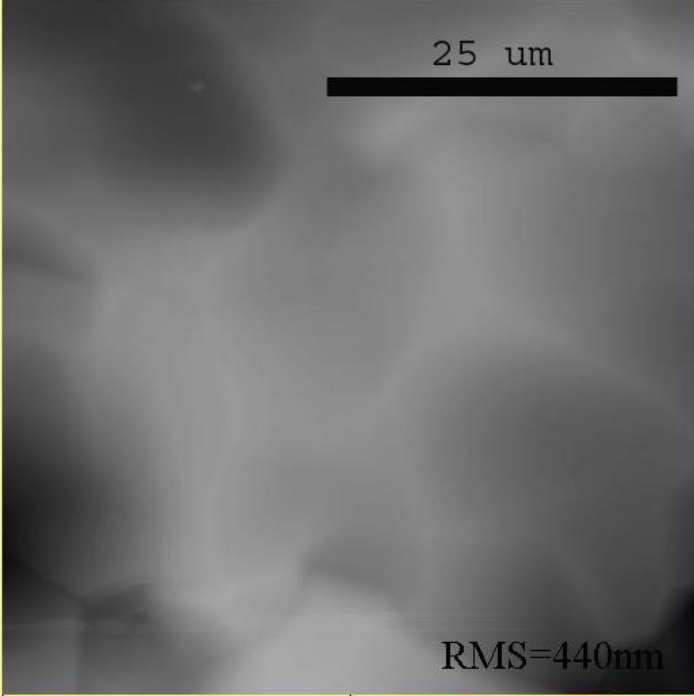


Fig.30d

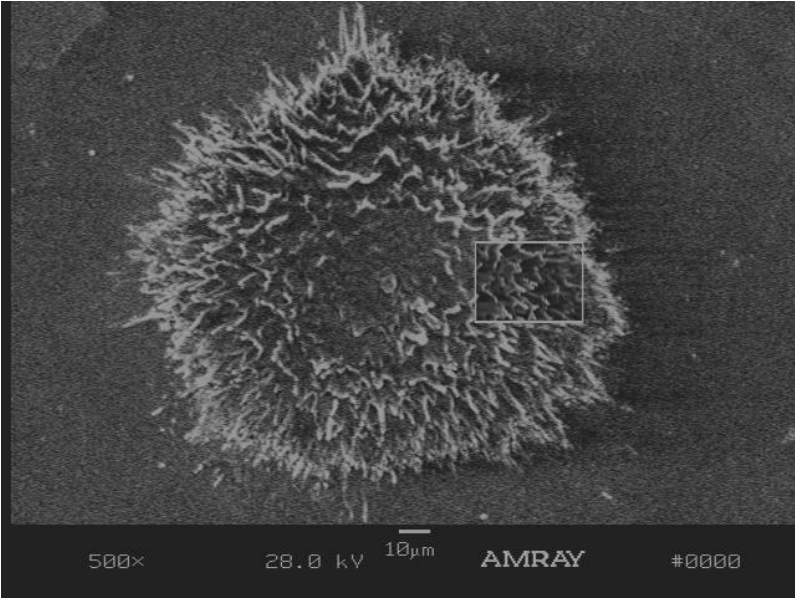


Fig.31

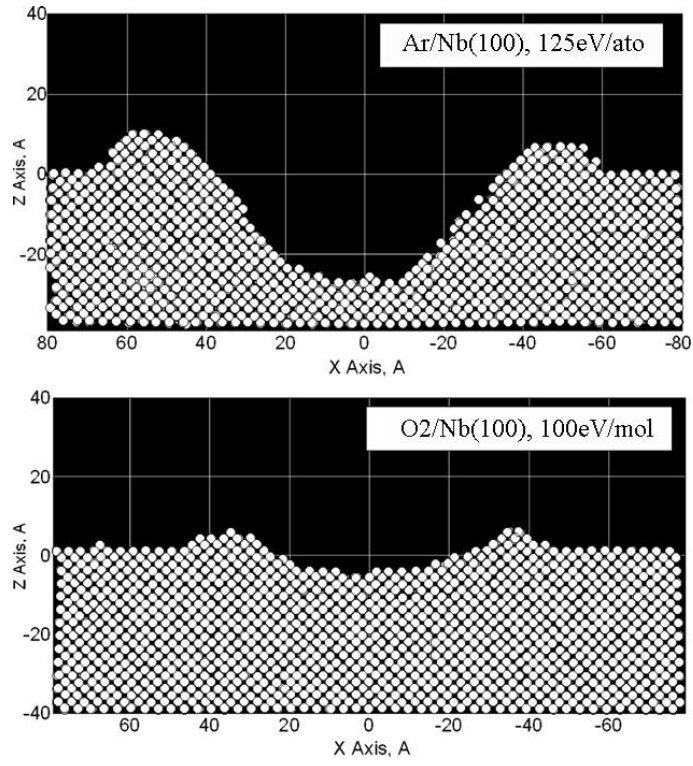


Fig.32

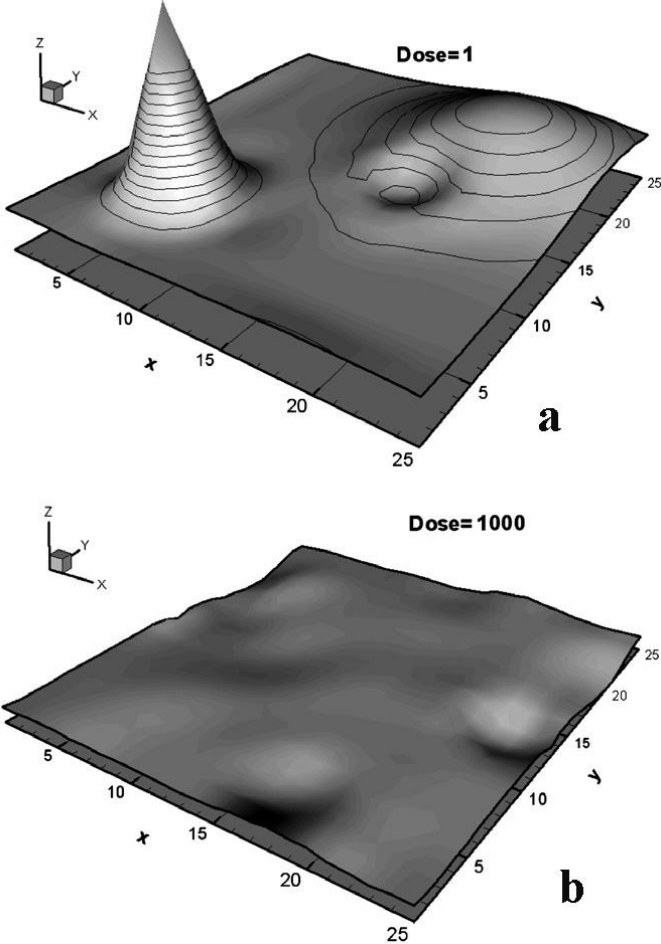


Fig.33

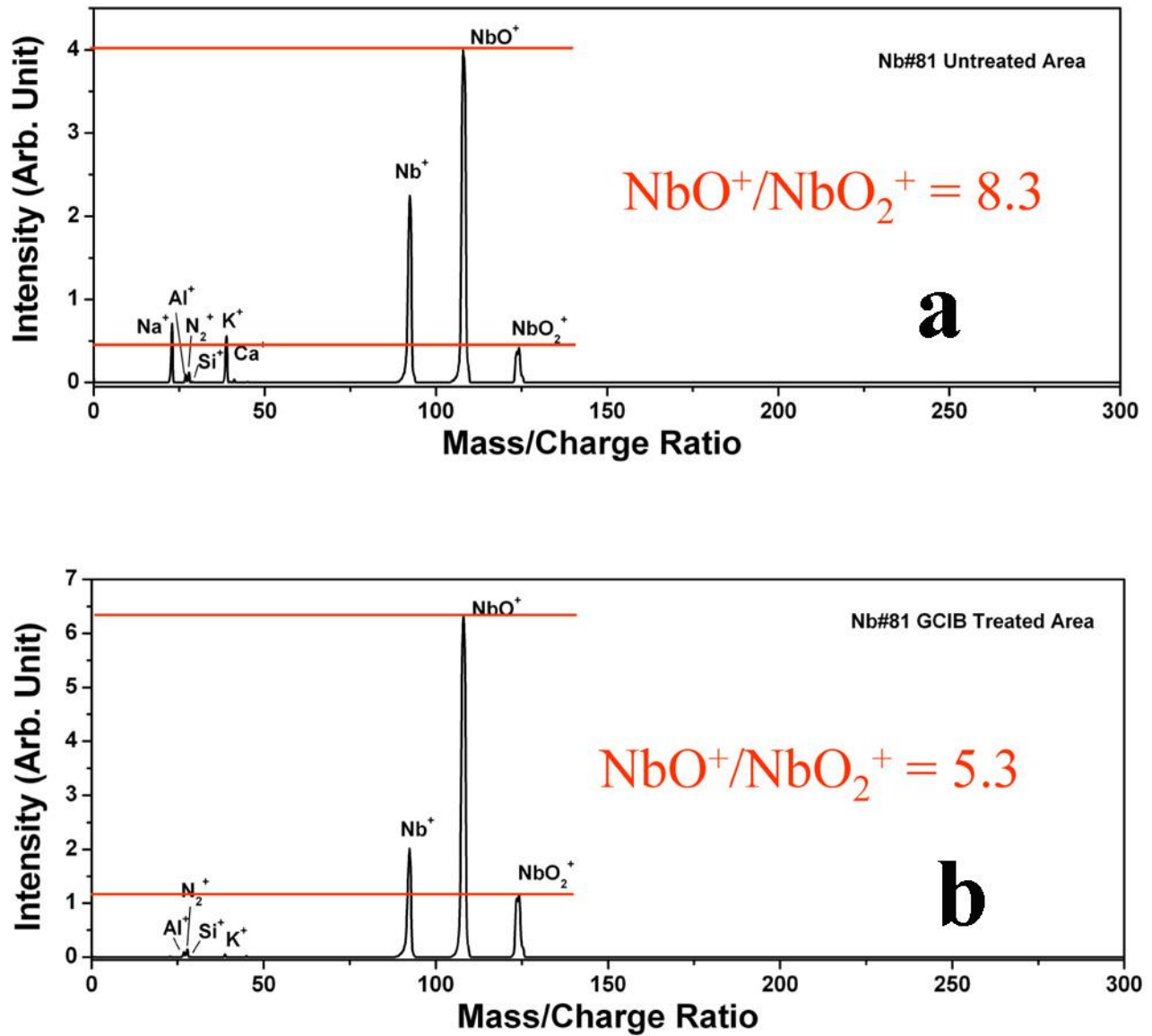


Fig.34

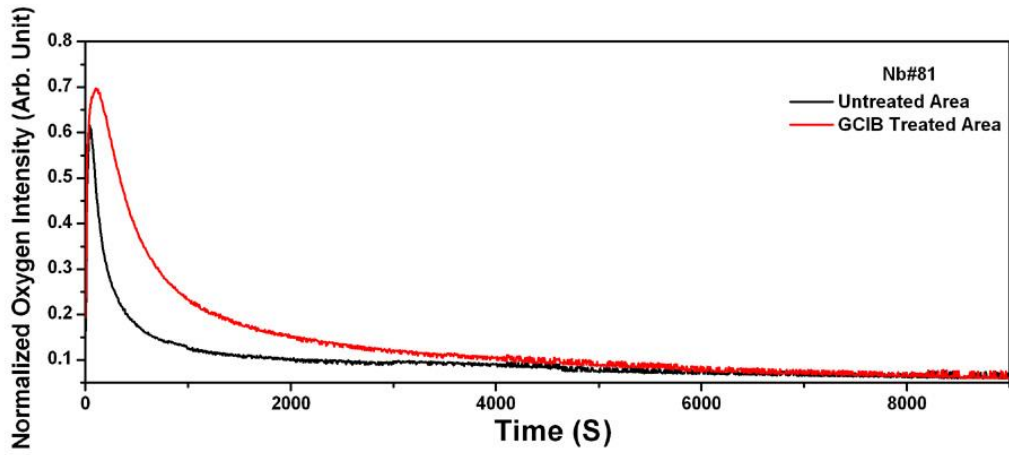


Fig.35

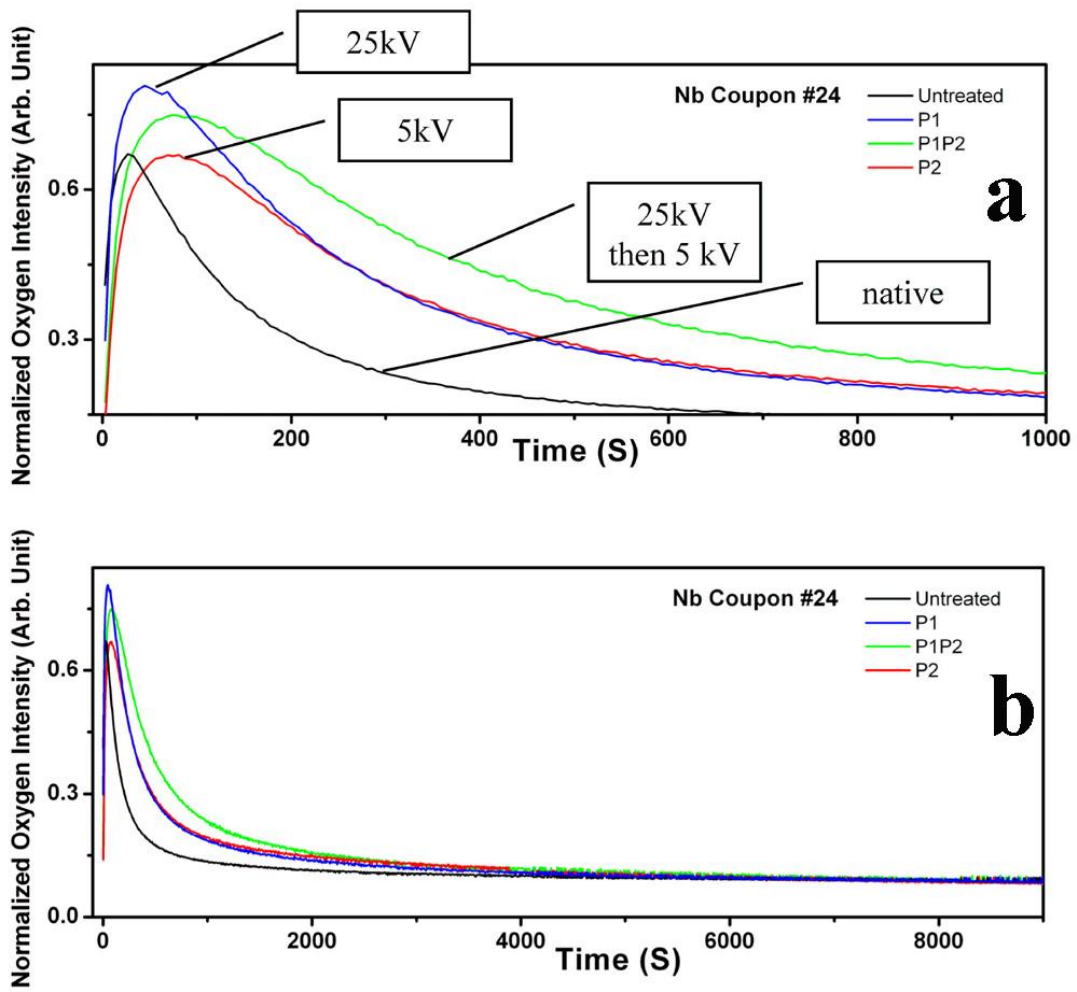


Fig.36

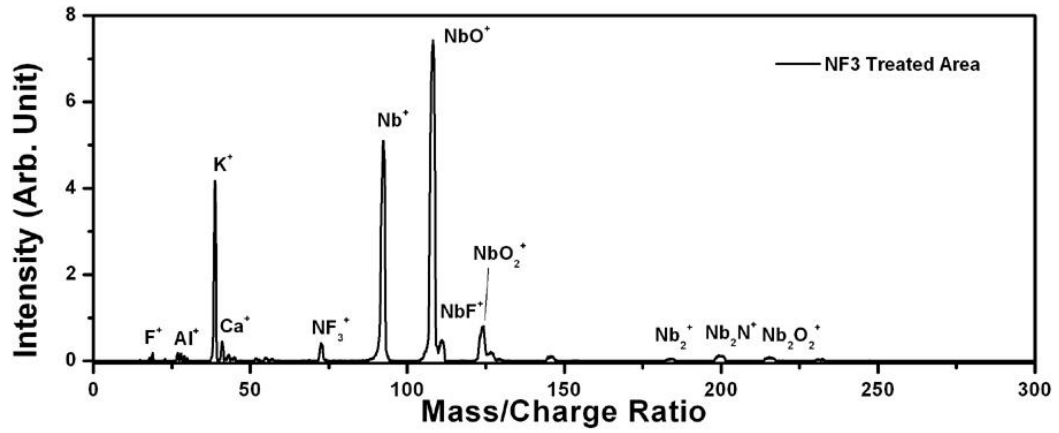


Fig.37

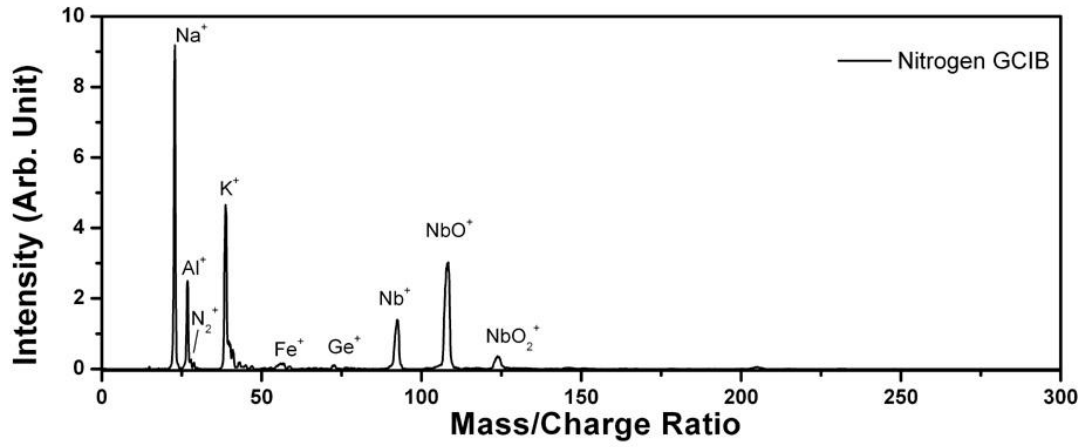


Fig.38

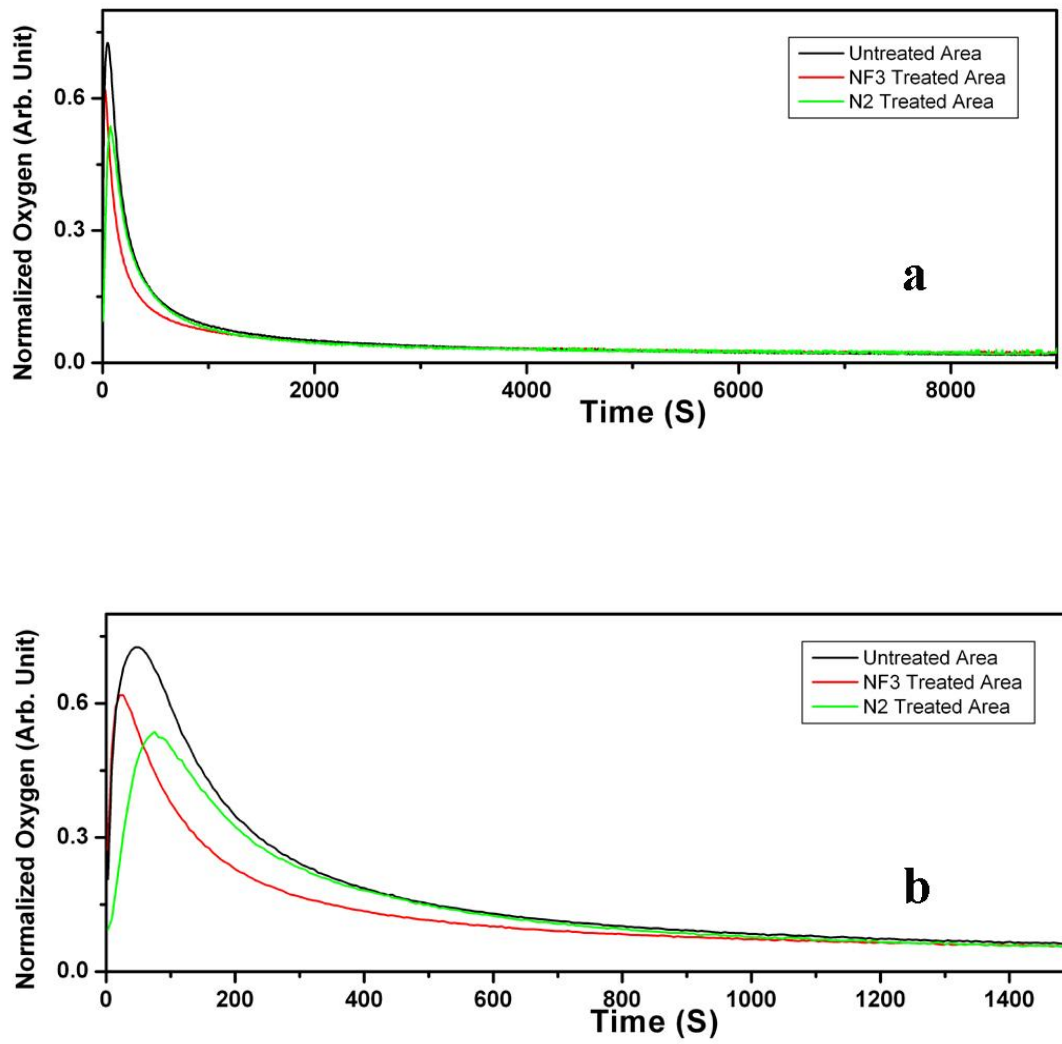


Fig.39

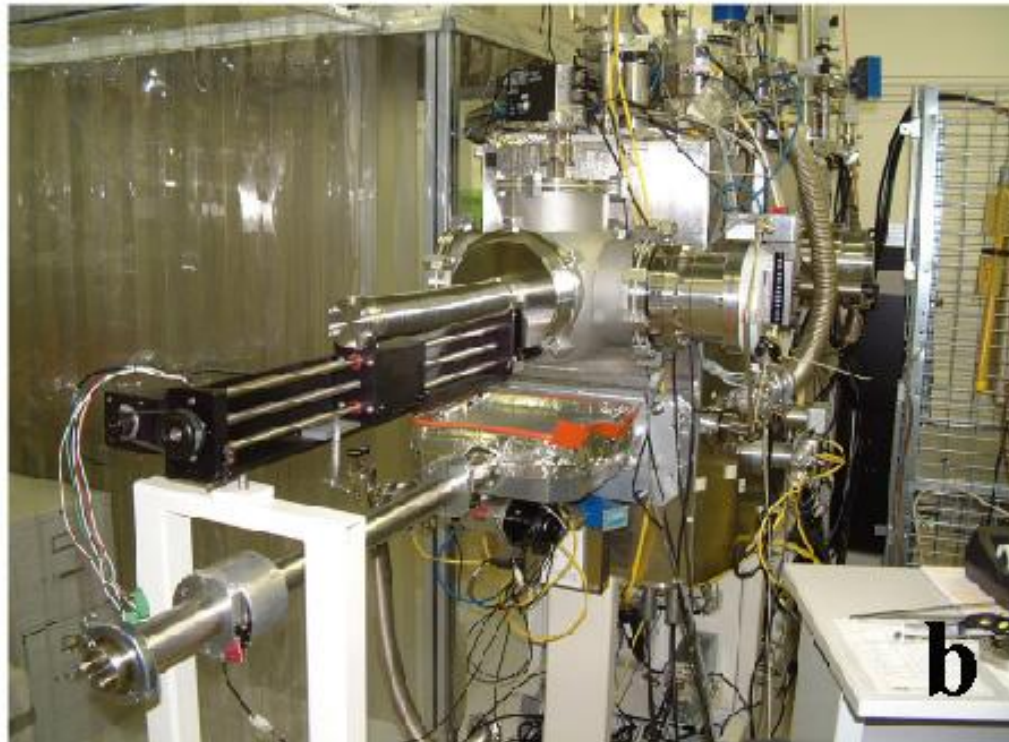
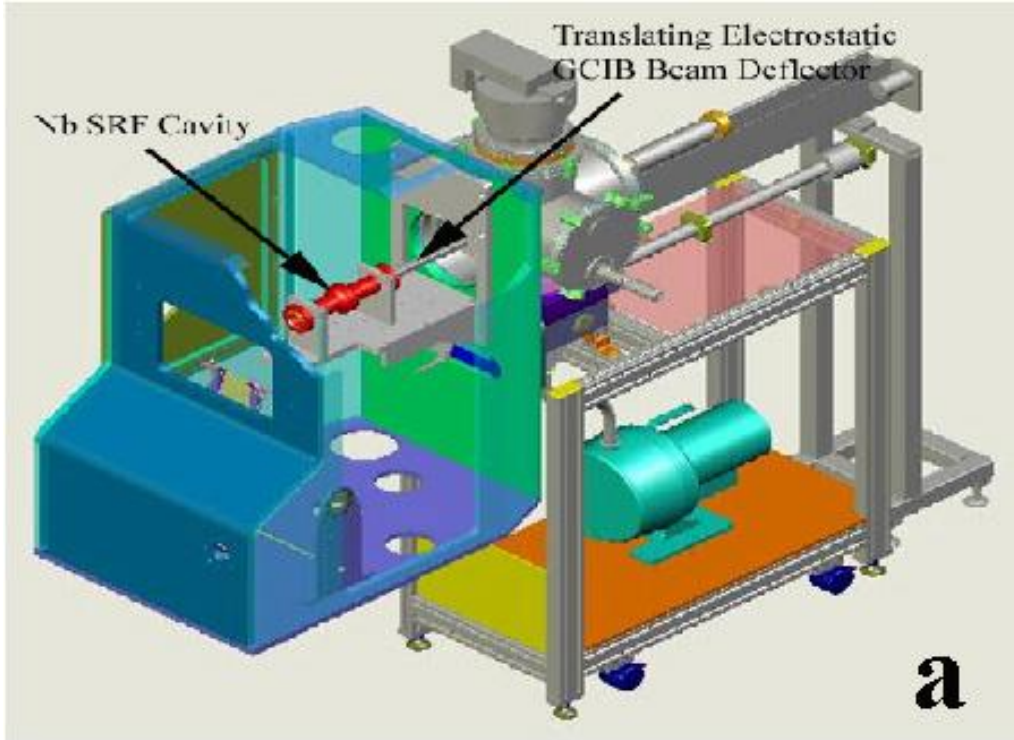


Fig.40

Design used for first test

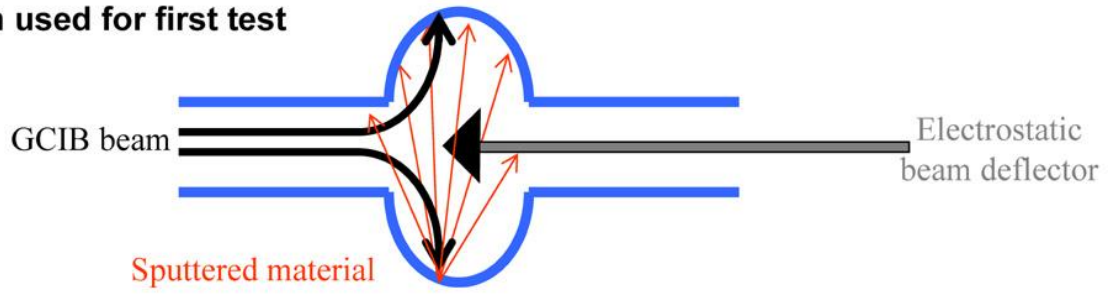


Fig.41

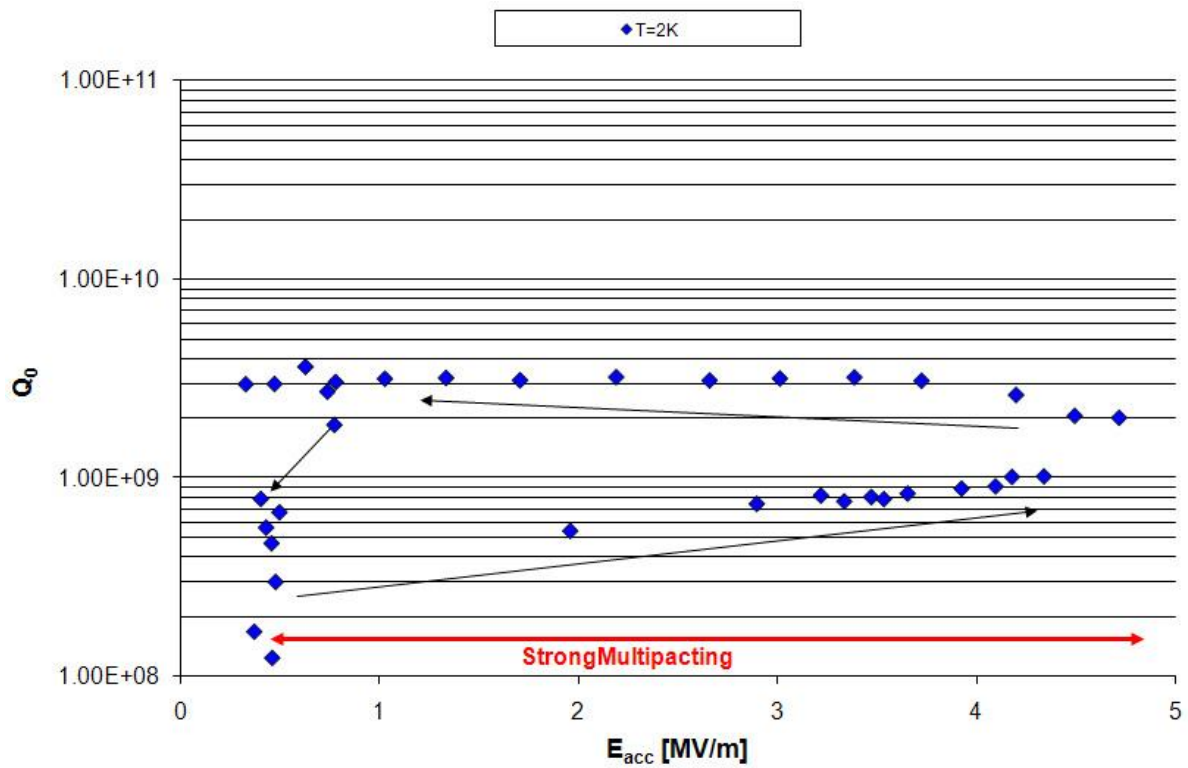


Fig.42

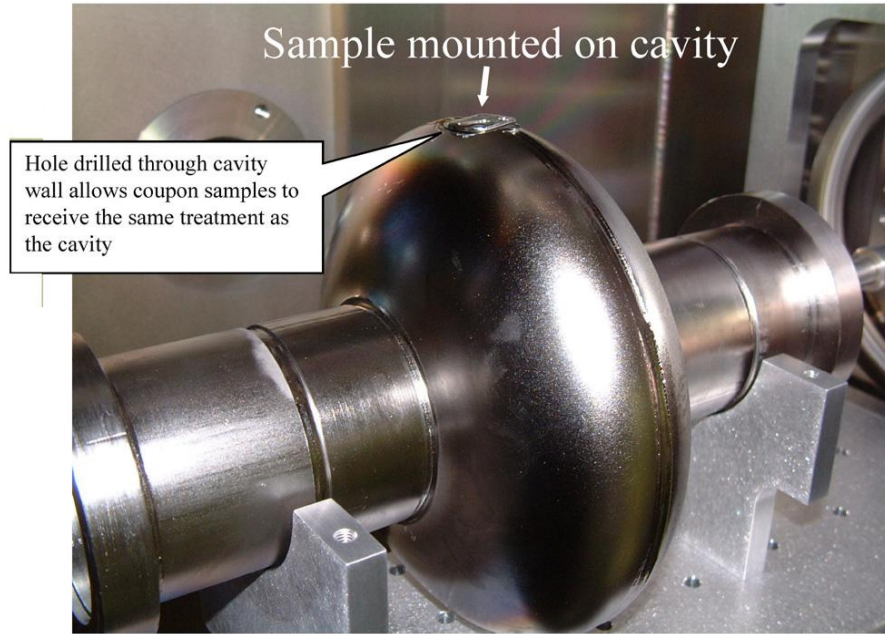


Fig.43

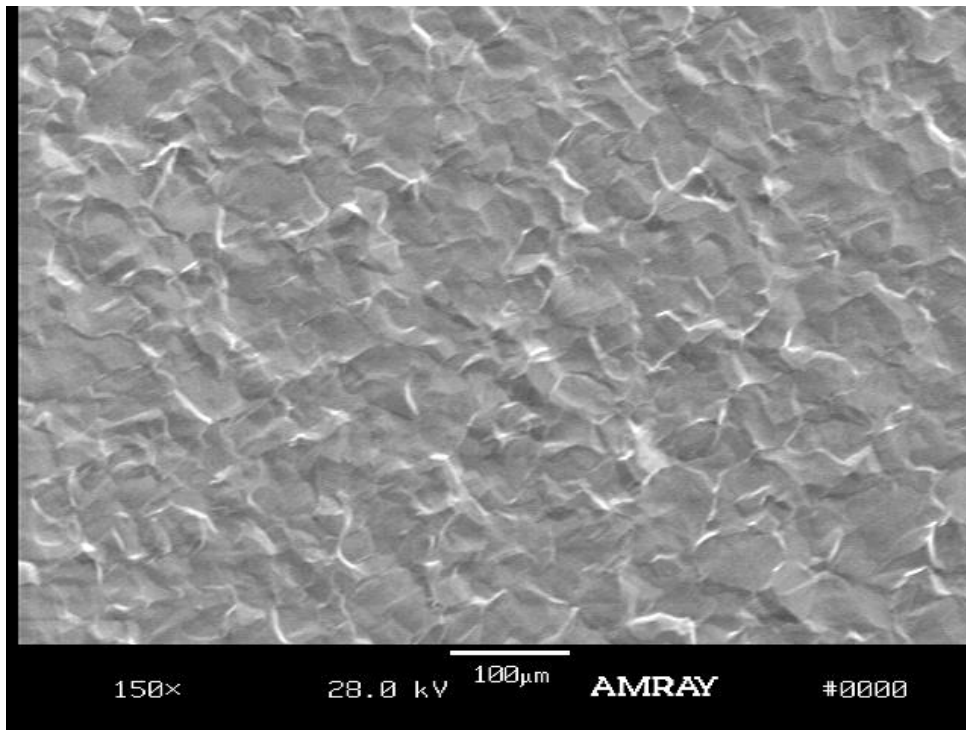


Fig.44

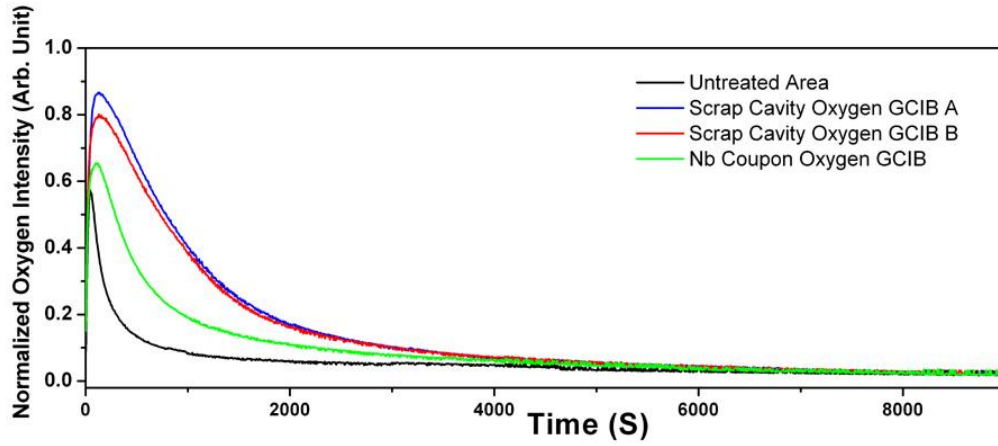


Fig.45

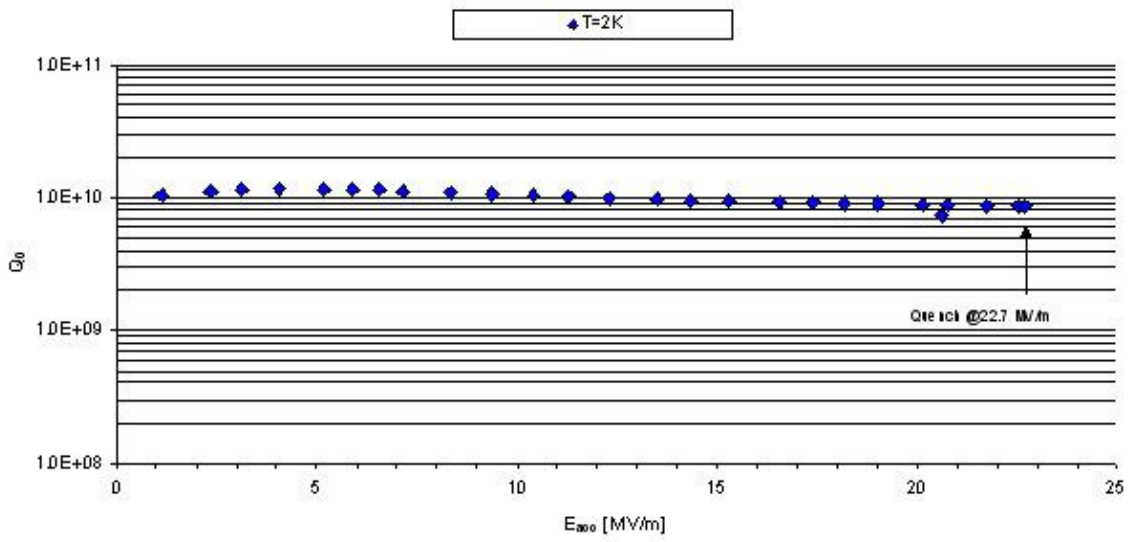


Fig.46

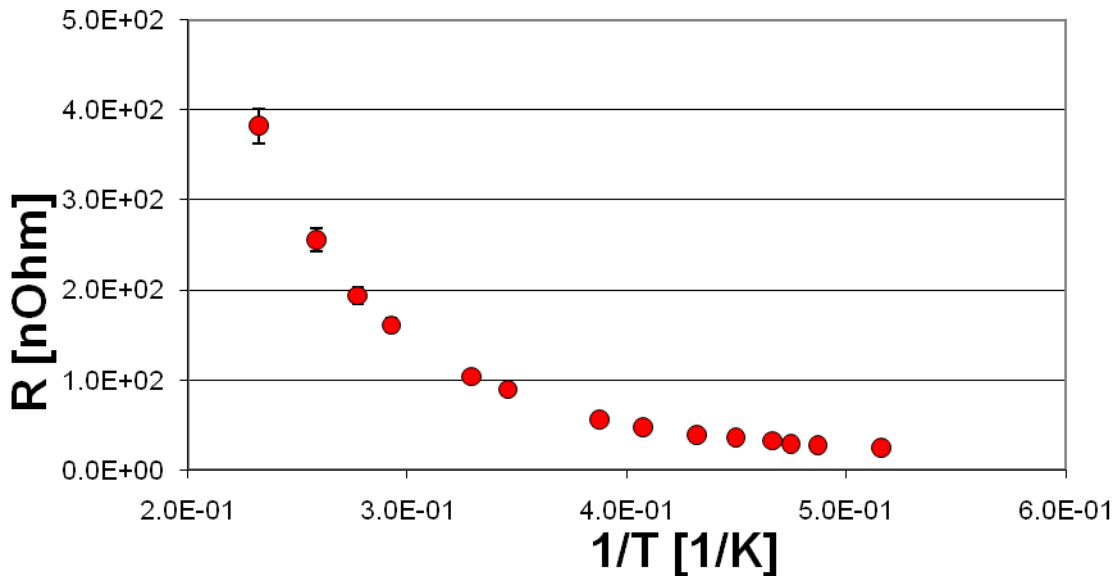


Fig.47

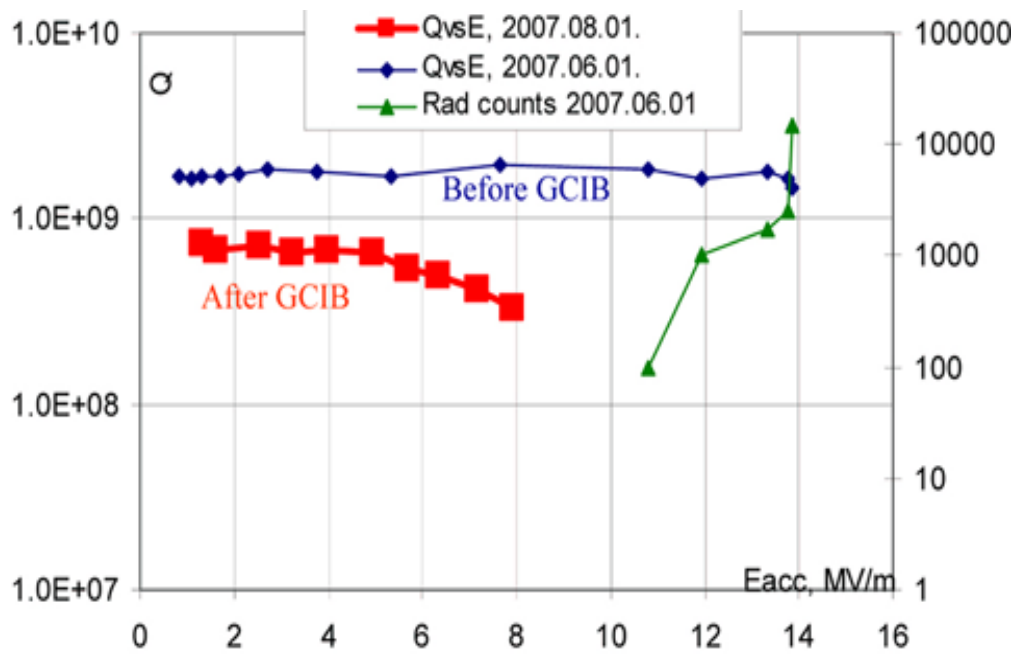


Fig.48

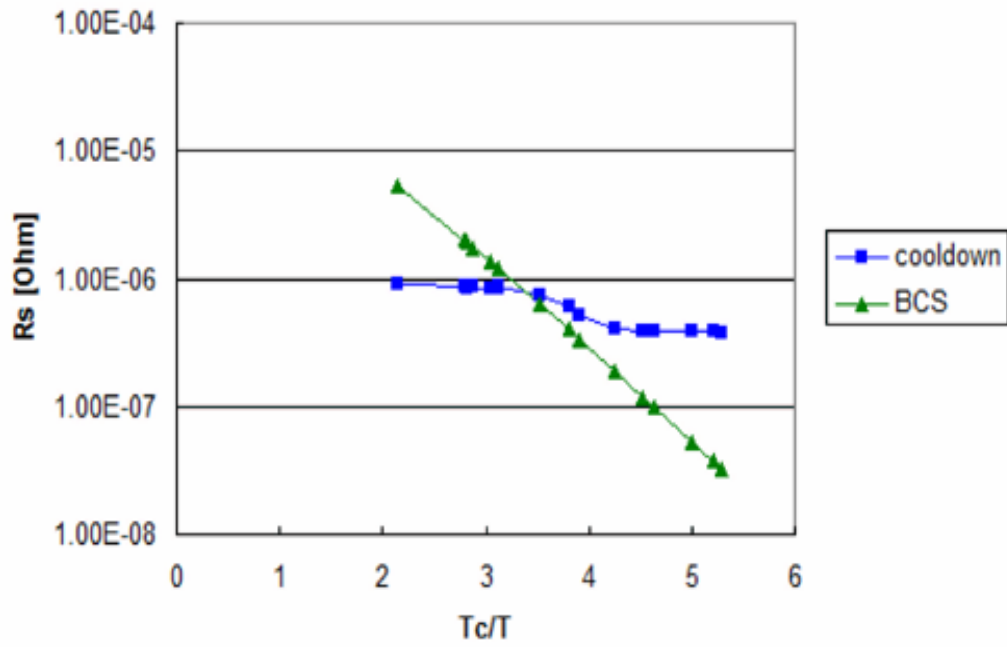


Fig.49

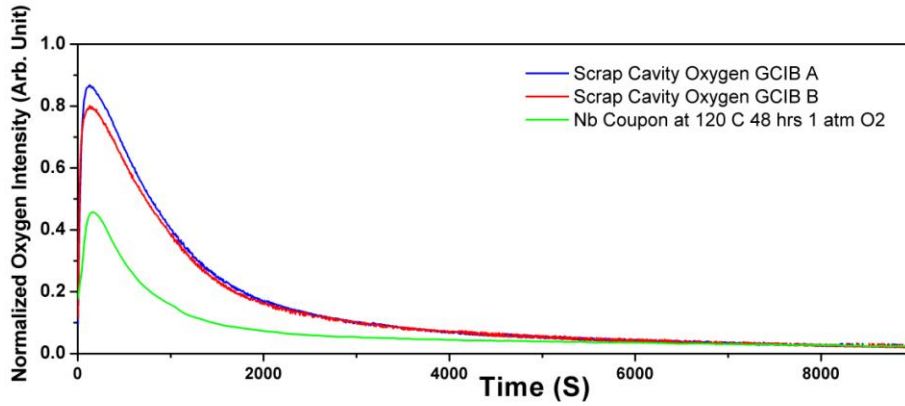


Fig.50

Proposed advance design

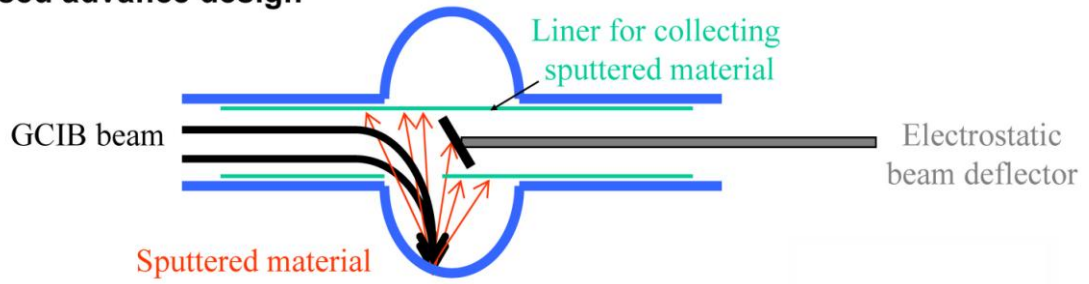


Fig.51

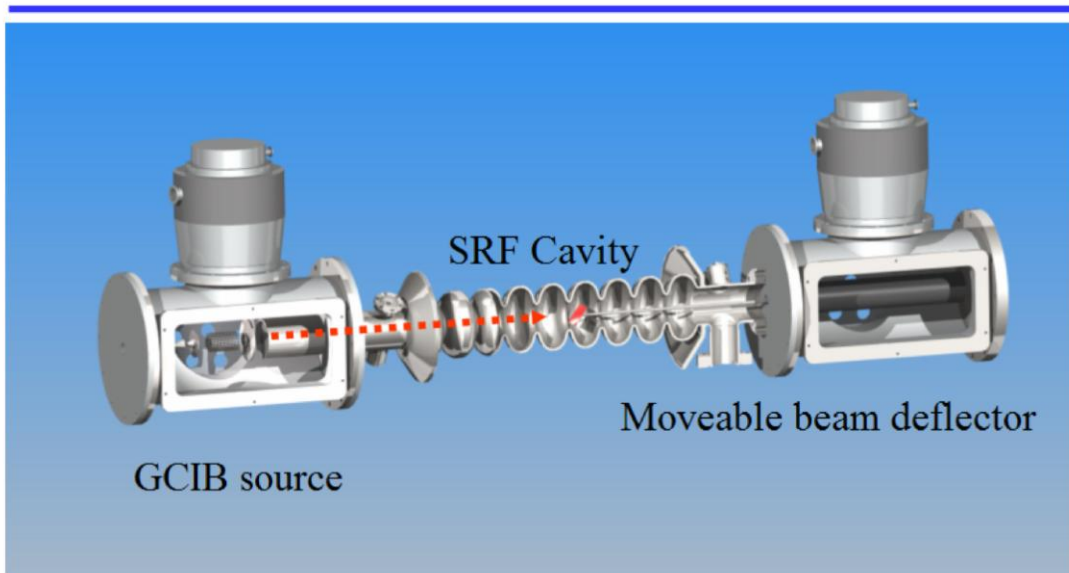


Fig.52